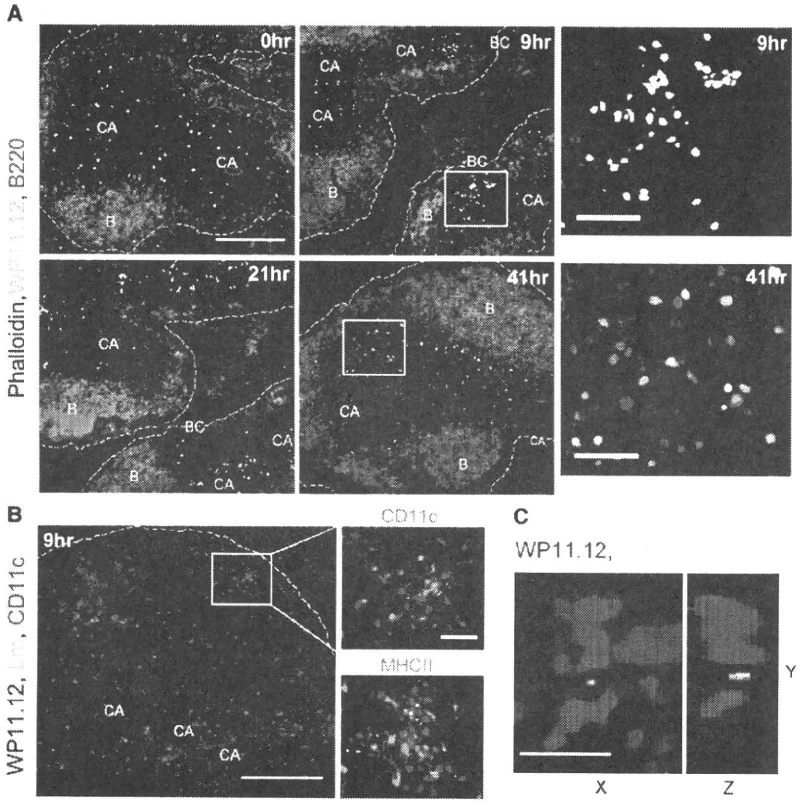

Figure 4. Antigen Presentation Kinetics and Location during Lm Infection in the Spleen

(A) CFSE-labeled WP11.12 CD8$^+$ T cells (4×10^6 cells, green) were adoptively transferred into mice before infection with 10^5 Lm. Spleens were harvested at the indicated times and stained with B220 to identify B cell follicles (red). White dashed lines indicate the edge of the white pulp based on phalloidin staining (blue). Scale bars represent 200 μm. Zoomed images (from white boxes) of WP11.12 cells in the PALS at 9 hr and 41 hr. Scale bars in zoomed images represent 50 μm. Figures are representative of more than five images per group from at least three independent experiments.

(B) Lm-specific T cell clusters (WP11.12, blue), CD11c$^+$ cells (red), and Lm (green) at 9 hr after infection. Scale bar represents 100 μm. Insets show zoomed in views of T cell clusters (blue) and CD11c or MHC II staining (red). Scale bar in zoomed image represents 20 μm. Images are representative of at least two independent experiments.

(C) 3D image of a representative Lm-specific T cell cluster (blue) ~10 hr after infection with 10^5 GFP-expressing Lm (cyan). BALB/c mice received 2×10^6 CMAC-labeled WP11.12 cells. Scale bar represents 20 μm.

be the primary APC type interacting with CD8$^+$ T cells in the early stages of infection.

Lm Transport to PALS Is Required for Antigen Presentation

We performed time-lapse 2P microscopy (Germain et al., 2006; Miller et al., 2002) to determine whether blocking Lm entry into the PALS with PTx would inhibit antigen presentation. Spleens were removed, secured to plastic coverslips with veterinary tissue adhesive, cut longitudinally with a vibrotome to expose the white pulp regions, and placed in warm oxygenated medium for imaging.

In uninfected mice, Lm-specific WP11.12 T cells moved randomly in the PALS with a median track velocity of ~5 μm min^{-1} and a motility coefficient of ~60 μm^{2}min^{-1}, similar to polyclonal CD8$^+$ T cells (Figures 5A and 5B; see also Movie S1). T cells migrated randomly and did not form clusters, similar to the T cell behavior previously observed in lymph nodes (Miller et al., 2002). However, the median T cell velocities measured in spleen explants were lower than mean values published for T cell migration in lymph nodes of ~12 μm/min (Miller et al., 2002). Our explanation for this discrepancy is that the decreased frame rate used in our current study (~2 images/min versus 4–6 images/min in previous studies) smoothes the characteristically large fluctuations in velocity associated with T cell motility and reduces the measured peak velocity in the data set. A decrease in peak velocity consequently yields a lower median velocity because the median is calculated from the velocity range. To investigate this issue further, we imaged T cells in explanted lymph nodes with our acquisition protocol and found slightly higher median T cell velocity (~7–8 μm/min, data not shown), suggesting that T cell motility is slightly slower in the spleen.

In infected mice, WP11.12 T cells showed significantly reduced velocity and motility (Figures 5A and 5B; see also Movie S2). Lm-specific T cells formed large aggregates in the PALS containing approximately 15 cells per cluster (Figures 4C and 5B). Occasionally, a few polyclonal CD8$^+$ T cells interacted transiently with the WP11.12 clusters, but most remained motile with no substantial reduction in velocity and motility (Figure 5B), indicating that cluster formation is antigen specific. Because the high antigen-specific T cell frequencies in adoptive transfer experiments can alter the kinetics and differentiation of responding T cells, we performed a limited number of experiments by using as few as 500,000 adoptively transferred Lm-specific T cells (Figure S6). Under these conditions we observed similar antigen recognition kinetics and clustering behavior (~4 cells per cluster; Figure S6; Movie S3).

When mice were pretreated with PTx to prevent Lm transport to the PALS, the clustering of bacteria-specific T cells was inhibited (Figures 5A and 5B; see also Movie S4). The lack of clustering was not due to the inhibition of T cell motility, because adoptively transferred polyclonal T cells moved with comparable velocity and motility in PTx-pretreated and untreated mice (Figures 5A and 5B) in our experimental protocol. When PTx was given ~2 hr after T cell adoptive transfer, we observed decreased T cell motility (data not shown), similar to the results of

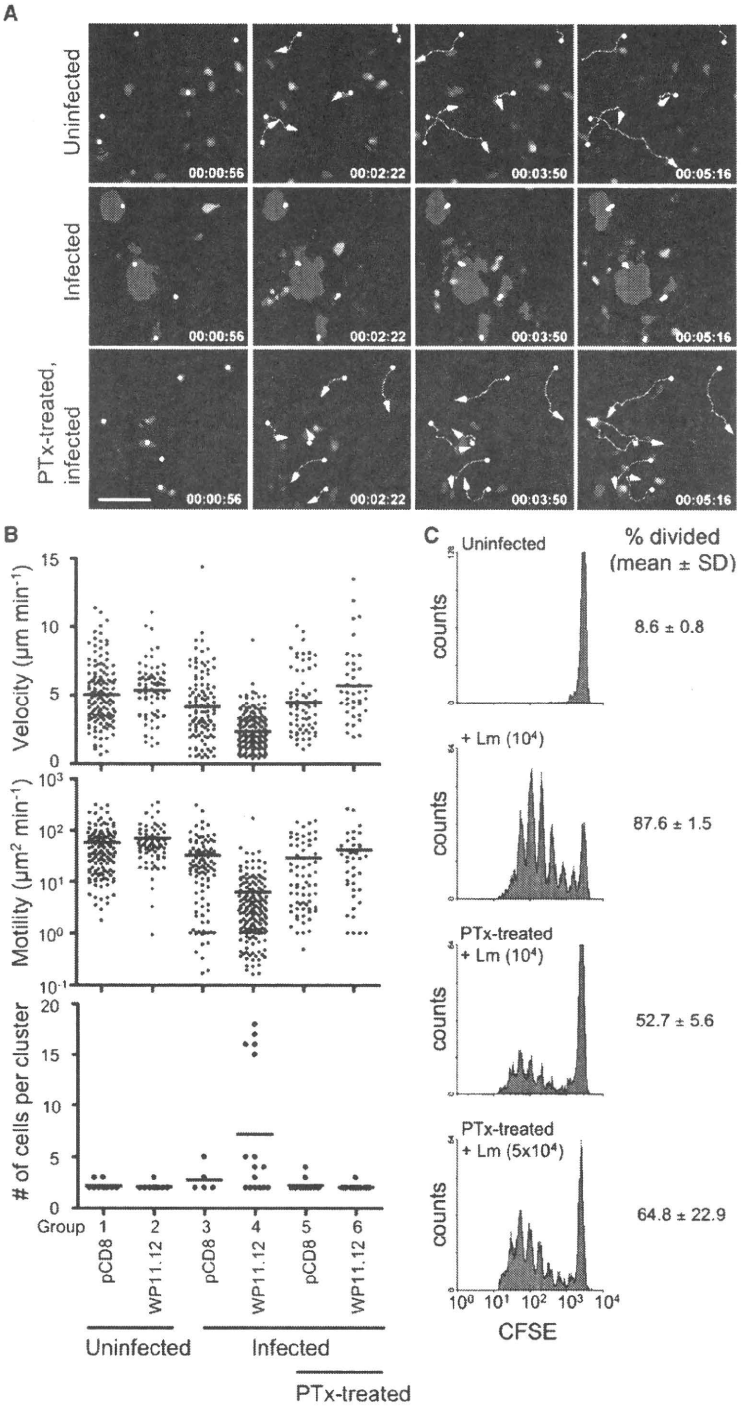

Figure 5. PTx Inhibits Antigen Presentation to Lm-Specific CD8⁺ T Cells

(A) 2P time-lapse image sequences of T cells ~9 hr after infection in explanted spleens. Lm-specific WP11.12 T cells (4–6 × 10^6, blue) and polyclonal CD8⁺ T cells (5–7 × 10^6, red) were transferred into naive mice or PTx-pretreated mice. 6 hr later, mice were infected with 10^5 Lm. Representative WP11.12 cell tracks are shown (yellow lines). Scale bar represents 20 μm.

(B) WP11.12 and polyclonal CD8⁺ T cell (pCD8) tracks were analyzed for velocity, motility, and cluster formation. Bars show means for each data group (1–6). Data are representative of at least three independent experiments. Median velocity: group 1 versus 2, $p > 0.05$; 3 versus 4, $p < 0.001$; 5 versus 6, $p > 0.05$; 2 versus 4, $p < 0.001$; 2 versus 6, $p > 0.05$; 3 versus 5, $p > 0.05$; 4 versus 6, $p < 0.001$. Motility coefficient: group 1 versus 2, $p > 0.05$; 3 versus 4, $p < 0.001$; 5 versus 6, $p > 0.05$; 2 versus 4, $p < 0.001$; 2 versus 6, $p < 0.05$; 3 versus 5, $p > 0.05$; 4 versus 6, $p < 0.001$. Cluster size: group 1 versus 2, $p > 0.05$; 3 versus 4, $p > 0.05$; 5 versus 6, $p > 0.05$; 2 versus 4, $p < 0.05$; 2 versus 6, $p > 0.05$; 4 versus 6, $p < 0.01$. p values were calculated with the Kruskal-Wallis test.

(C) 5–7 × 10^6 CFSE-labeled WP11.12 T cells were adoptively transferred into mice. T cell proliferation was measured in uninfected control mice and on day 3 after infection in three experimental groups: mice infected with 10^4 Lm, mice pretreated with PTx then infected with 10^4 Lm, and mice pretreated with PTx and infected with 5 × 10^4 Lm (a five times higher dose was used in this group in order to compensate for the reduced Lm burden in the PTx-treated mice). PTx reproducibly inhibited Lm-specific T cell proliferation but did not completely block it. The mean ± SD of three mice in one representative experiment is shown. Data are representative of at least three independent experiments with similar results.

others (Huang et al., 2007). This suggests that although PTx is capable of inhibiting T cell migration in the spleen, it does not remain active 24 hr after injection. As a further control for potential PTx effects on T cells, we administered PTx after Lm had entered the PALS (9–10 hr after infection). Lm-specific and polyclonal T cells were transferred and 2 hr later spleen explants were examined by 2P microscopy. Once Lm transport had occurred, PTx treatment no longer inhibited WP11.12 cluster formation whereas control T cells showed normal motility (Movie S5). Although Lm could be detected in the MZ and RP of PTx-treated mice (Figure 1D), we did not detect T cell clusters in these regions (Figure 4; 2P data not shown).

As a second indicator of antigen presentation, we measured adoptively transferred WP11.12 T cell proliferation by CFSE dilution assay. PTx pretreatment reproducibly decreased the number of proliferating WP11.12 T cells compared to untreated controls (Figure 5C). Decreased T cell proliferation was also observed when a larger inoculum of Lm was used to compensate for the lower Lm CFU present in PTx-treated mice at 24 hr (Figure 5C, bottom). We also assessed the effects of PTx treatment on antigen presentation in vitro by using the Ova-specific OT1 transgenic T cells. DC were isolated from spleen and treated in vitro with 20 and 200 ng/ml Ptx for 2 hr (200 ng/ml is roughly equivalent to the in vivo dose of 500 ng per mouse.). After PTx treatment, DC were fed OVA or OVA-conjugated beads in the presence of LPS for 4 hr before coculture

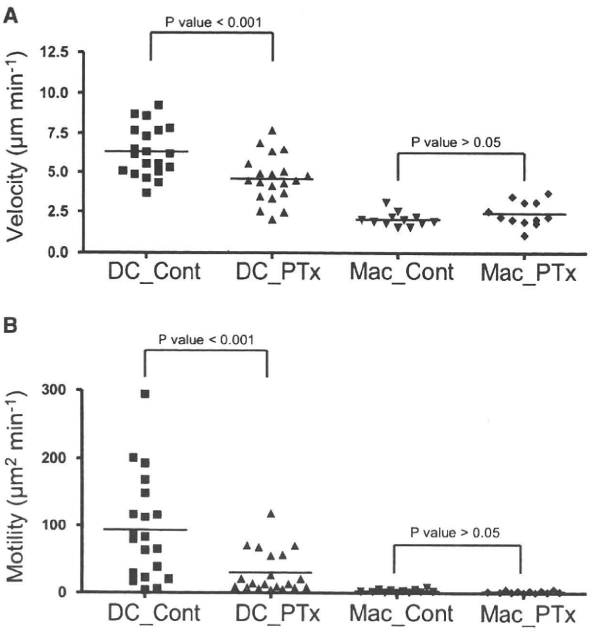

Figure 6. PTx Effects on DC and Macrophage Motility In Situ

Spleen explants were prepared (as described in Experimental Procedures) from CD11c-YFP mice (Lindquist et al., 2004) that received PBS or 500 ng of PTx 24 hr earlier. Spleen explants were imaged with 2P microscopy and cell motility analyzed (see Experimental Procedures for details).

(A) Median track velocity.

(B) Motility coefficient of DCs and macrophages (Mac) was determined. PTx significantly reduces DC motility and probing behavior but has no observable effect on macrophages, which are normally not motile in our time-lapse images. The data were generated from three independent experiments per group. One-way analysis of variance with Newman-Keuls Multiple Comparison post test was performed.

The p values for (A) are: Mac PTX versus DC_Control, $p < 0.001$; Mac_PTX versus DC_PTX, $p < 0.001$; Mac_PTX versus Mac_Control, $p > 0.05$; Mac_Control versus DC_Control, $p < 0.001$; Mac_Control versus DC_PTX, $p < 0.001$; DC_PTX versus DC_Control, $p < 0.001$. The p values for (B) are: Mac_PTX versus DC_Control, $p < 0.001$; Mac_PTX versus DC_PTX, $p > 0.05$; Marc_PTX versus Mac_Control, $p > 0.05$; Mac_Control versus DC_Control, $p < 0.001$; Mac_Control versus DC_PTX, $p > 0.05$; DC_PTX versus DC_Control, $p < 0.001$.

with OT1 T cells for 3 days. Ptx had no detectable effect on antigen presentation with either OVA or OVA-conjugated beads (Figure S7).

Next, we examined the effect of PTx treatment on the behavior of resident DCs and macrophages by using 2P microscopy. CD11c-YFP mice (Lindquist et al., 2004) were given a single i.p. injection of PTx (500 ng) 1 day before the spleens were harvested and prepared for time-lapse imaging. Fluorescent beads were injected i.v. to define the MZ and distinguish YFP^+ MZMs (containing many beads) from DCs (containing few or none) in our analysis. In mock-treated mice, DCs showed active probing behavior and appeared to migrate randomly in the PALS and bridging channel with a median velocity of 6.3 μm/min (Movie S6 and Figure 6). We also observed DCs migrating to and from the MZ-PALS border. In Ptx-treated mice, DC probing behavior was lost and cell velocity was significantly reduced ($p < 0.001$,

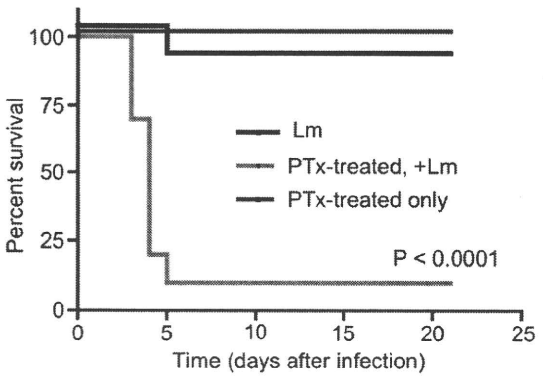

Figure 7. PTx Treatment Decreases the Survival of Mice after Lm Infection

Mice were pretreated with PTx i.p. then challenged with 5×10^3 Lm EGD. Survival was followed for 21 days. p values were calculated with a log rank test (n = 10 mice per group). Black line, infected mice; red line, PTx-treated, infected mice; blue line, PTx-treated, uninfected mice. Ptx treatment severely compromised the host responses to Lm infection.

Movie S7 and Figure 6A). Although DCs were able to move slightly, they exhibited little displacement over time and their motility coefficient was significantly reduced ($p < 0.001$, Figure 6B). PTx treatment did not appear to alter the behavior of MZMs and these cells remained essentially nonmotile over the time frame of our imaging experiments (Movies S6 and S7 and Figure 6).

During sublethal Lm infection, T cell responses reduce the bacterial burden 5–7 days after challenge and over 2 weeks, resulting in the eradication of Lm. We tested whether blocking Lm entry to the PALS with PTx affected the survival of mice to primary infection. Although PTx-treated mice had reduced CFU in the spleen at 24 hr (Figure 1E), these mice could not control Lm at later times and succumbed to infection (Figure 7). Because endogenous lymphocytes are presumably exposed to PTx in these experiments, it is unclear whether PTx affects survival by inhibiting antigen presentation to $CD8^+$ T cells or by inhibiting cell effector functions. Moreover, the decreased survival of PTx-treated mice could be due to the defective recruitment of TipDCs, which have been shown to be required to control Lm infection (Serbina et al., 2003).

DISCUSSION

In this study, we sought to determine whether DCs play a role in transporting bacteria from the MZ to the PALS, analogous to their role in carrying antigens from peripheral tissues to draining lymph nodes. The location and kinetics of bacterial antigen presentation in the spleen are poorly defined. 2P microscopy allowed us to assess antigen presentation in situ by quantifying changes in the motility and clustering of Lm-specific T cells. In the Lm infection model, we did not find evidence of bacteria-specific $CD8^+$ T cell responses in either the MZ or RP during the first 2 days of infection, suggesting that the PALS is the primary compartment where $CD8^+$ T cells first recognize antigen. In our study, we focused on the earliest detectable stages of antigen presentation. However, work with MHC class I tetramer staining in situ

showed that CD8$^+$ T cells clustered at the T cell-B cell zone border and MZ beginning 3 days after infection (Khanna et al., 2007), suggesting that other regions of the spleen are involved at later times. Moreover, T cell responses were detected in the splenic RP after an i.v. injection of soluble peptide (Odoardi et al., 2007), demonstrating that antigen presentation can occur outside the PALS. To what extent immune responses to viruses and other bacteria are initiated in distinct splenic compartments is an interesting question. If the location of antigen presentation is dependent on the type and route of infection, then the tissue microenvironment where antigen presentation occurs might play a pivotal role in shaping the character of the pathogen-specific immune response.

Our primary evidence linking Lm transport to antigen presentation is that PTx treatment inhibits both the entry of bacteria into the PALS and the recognition of bacterial antigen. We used 2P imaging to analyze Lm-specific T cell responses and found that PTx inhibited the clustering and arrest of T cells only if administered before Lm gained entry into the PALS. We found that PTx treatment after T cell adoptive transfer does indeed decrease T cell velocity in the spleen, as observed by others (Huang et al., 2007; Okada and Cyster, 2007). However, in our protocol, the inhibition of antigen presentation by PTx is due to blocking APC migration and not due to inhibition of T cell motility, because adoptively transferred T cells appear unaffected (i.e., motility was identical in PTx-treated and untreated mice). Moreover, when we gave PTx 2 hr before T cell transfer, control T cells showed normal motility and Lm-specific T cells clustered normally. Our explanation is that PTx is rapidly consumed in vivo and does not affect T cells transferred subsequently.

Our 2P microscopy experiments revealed that PTx markedly inhibited DC motility in the spleen. Previously, PTx was reported to inhibit DC homing to the thymus, but not the spleen (Bonasio et al., 2006). Although DCs may enter the spleen passively from the circulation, DC migration into the PALS appears to require chemokine receptor signaling, as suggested by studies with CCR7-deficient knockout mice (Kursar et al., 2005).

There were no statistical differences in CFU counts per spleen between Ptx-treated mice and untreated controls during the first 6 hr of infection, suggesting that PTx treatment did not interfere with the initial trapping of Lm. However, the increased CFUs in PTx-treated mice at 24 hr indicated that the infection does not progress normally and that Lm proliferation in the PALS is inhibited. Although PTx could interfere with actin rearrangements involved in the host cell invasion by Lm or cell-cell spread, we believe that the main effect of PTx is on splenocyte migration because others have shown that ActA-deficient Lm were capable of invading and proliferating in the PALS, albeit at a lower level (Muraille et al., 2005). Moreover, we performed histological experiments to examine the impact of PTx pretreatment on Lm capture and found that the cellular distribution and amount of bacteria captured was similar to untreated control mice.

Neuenhahn et al. (2006) concluded that viable Lm was found exclusively in CD8α^+ DCs 3 hr after infection and proposed that these DCs were responsible for the initial trapping of live Lm in the spleen. Our results extend on previous work by showing that DCs facilitate Lm entry into the PALS and that this entry is required for efficient antigen presentation. It is noteworthy that we found infected MOMA-1$^+$ macrophages and CD11b$^+$ cells in the PALS at 24 hr, but did not find CD8$^+$ T cell clusters associated with these cells, and therefore their role in antigen presentation remains unclear. A variety of splenic phagocytes capture Lm initially, but bacteria expand transiently in DCs, suggesting that DCs may support Lm growth in vivo (unpublished observations). It is possible that the transient proliferation of bacteria in DCs is advantageous to host survival because it would be expected to provide abundant cytosolic antigen to stimulate CD8$^+$ T cell-mediated immunity.

The role of different DC subsets in Lm pathogenesis and antigen presentation is a key question that is difficult to address because current methods for DC ablation, such as the CD11c-DTR system, deplete all CD11c$^+$ DCs, as well as splenic macrophages (Probst et al., 2005). The spleen contains two main DCs subsets, CD8α^+DEC205$^+$ DCs, which reside in the PALS and bridging channel (Steinman et al., 1997) and present MHC I bound peptides more efficiently (Dudziak et al., 2007), and CD8α^-, 33D1$^+$ DCs found primarily in the RP and MZ (Steinman et al., 1997), which present antigen to CD4$^+$ T cells preferentially. Neuenhahn et al. (2006) observed CD8α^+ DCs in the MZ and RP where they would have direct contact with Lm entering the spleen. Although CD8α^+ DCs were shown to preferentially contain live Lm, DCs were not strictly required for antigen presentation because the adoptive transfer of infected macrophages could restore T cell responses in mice depleted of DCs (Neuenhahn et al., 2006). CD8α^+ DC have been shown to prime T cell responses to Lm (Belz et al., 2005), suggesting that these DCs play a central role in stimulating Lm-specific responses. Moreover, CD8α^+ DCs are specialized for crosspresentation (den Haan et al., 2000) and this function may be important for stimulating T cell responses to Lm. In our study it is noteworthy that we often found T cell clusters around infected DCs, suggesting that early CD8$^+$ T cell activation proceeds primarily via the classical MHC I pathway. We did not examine MHC II antigen presentation and it is entirely possible that different regions of the spleen and distinct APCs might be involved in activating CD4$^+$ T cells (Odoardi et al., 2007).

Defining the precise cellular mechanisims that deliver bacterial antigens to the PALS is important for understanding how antigen presentation occurs in the spleen. Recently, Cinamon et al. (2008) showed that MZ B cells shuttle soluble antigen from the MZ to follicles in the white pulp in a CXCR5-dependent manner. Because the entry of Lm into the PALS is sensitive to PTx treatment, bacterial transport likely involves chemokine signaling as well. CCR7-deficient mice showed decreased T cell priming and increased susceptibility to Lm infection (Kursar et al., 2005). This result was attributed to the failure of T cells and DCs to efficiently colocalize in the absence of CCR7; however, this study did not address the impact of CCR7 deficiency on Lm transport and antigen presentation directly. The work of others suggests that the transport of Lm to the PALS is contingent on the cytosolic entry of bacteria given that neither heat-killed nor LLO-deficient Lm enter the host cell cytosol and both fail to reach the PALS after i.v. challenge (Glomski et al., 2003; Lauvau et al., 2001; Muraille et al., 2005). Importantly, these non-cytosolic forms of Lm also fail to elicit robust T cell immunity, suggesting a link between PALS infection and T cell priming. As suggested by Muraille et al. (2005), a critical step in the progression of Lm infection to the PALS might be the recognition

of bacteria by intracellular sensors such as the NOD-like receptors (Mariathasan and Monack, 2007; Dufner et al., 2007; Park et al., 2007).

There are several plausible mechanisms for Lm entry to the PALS: migration of infected DCs from MZ to PALS, migration of PALS DCs to the MZ boundary to capture and carry back Lm, and cell-cell spread of Lm from MZ to PALS. The issue of cell-cell spread has been addressed by experiments with ActA-deficient Lm, which cannot mobilize host cell actin (Muraille et al., 2005). In the presence of gentamicin, ActA-deficient Lm can still enter the PALS, arguing that PALS infection does not require cell-cell spread. Ideally, single-cell tracking experiments with GFP-Lm and 2P microscopy will help determine whether one or more of these mechanisms is at work.

We propose that early host-pathogen interactions in the MZ lead to the transport of intracellular antigen to the PALS for presentation to T cells. Our results with Lm suggest that targeting antigen delivery to the PALS might be an effective strategy to enhance vaccine efficacy and the priming of $CD8^+$ T cells to intracellular pathogens.

EXPERIMENTAL PROCEDURES

Mice

BALB/cJ mice were obtained from The Jackson Laboratory. CD11c-YFP mice (Lindquist et al., 2004) were a gift of the M. Nussenzweig lab. WP11.12 TCR transgenic mice, expressing a transgenic TCR that recognizes $p60_{449-457}$ peptide in the context of H-$2K^d$ (Mercado et al., 2000), were a gift from E. Pamer (Sloan-Kettering Institute, NY). Mice were maintained and bred under SPF conditions in the Washington University mouse facility.

Bacteria, Fluorescent Beads, and Dextran

The GFP-expressing Lm EGD strain was made with the pNF8 vector (Fortinea et al., 2000). The LD_{50} of our GFP-expressing Lm strain was 1.1×10^5 in BALB/c mice, or ~50-fold attenuated compared with wild-type EGD. Both GFP-expressing Lm and the EGD strain were stored as frozen glycerol stocks (~1×10^9/ml) at −80°C. Mice were infected with Lm diluted in PBS (to indicated doses) from frozen stocks or overnight cultures. For infection times less than or equal to 2 hr, we typically used 10^7 EGD Lm. For infections at 12 and 24 hr, we used 10^4–10^5 bacteria. FluoSpheres carboxylate-modified microspheres (yellow-green, 1.0 μm and 0.5 μm) and Fluorescein-conjugated dextran (lysine-fixable, 500 kD) were purchased from Invitrogen. All reagents were injected i.v. in a volume of 200 μl.

Histology

Mice were euthanized and spleens harvested and embedded in Tissue-Tek OCT compound. 5 μm cryosections were cut and fixed with 4% paraformaldehyde in PBS (pH 7.2) at 4°C for 5 min and then blocked with StartingBlock Blocking Buffer (PIERCE) for 10 min before being sequentially incubated with fluorescent dye-conjugated or biotin-conjugated primary antibodies (1:100 dilution with blocking buffer), fluorescent dye-conjugated secondary antibodies and/or fluorescent dye-conjugated streptavidin (1:100 dilution with blocking buffer). Sections were mounted in GVA mount (Invitrogen) and stored at 4°C. Details for antibodies and reagents used for immunofluorescence staining can be found in the Supplemental Data.

Immunofluorescence Microscopy

Four-color fluorescence microscopy of cryosections was performed with an Olympus BX51 equipped with 100W mercury lamp (Olympus) and a SPOT RT CCD camera (Diagnostic Instruments). Monochrome images (1200 pix × 1600 pix = 885 × 1180 μm with 10× objective; 440 × 586 μm with 20× objective, 12-bit depth) were acquired through fluorescence filters optimized for DAPI, FITC, TRITC, and Cy5 (Chroma). Images were acquired, processed to reduce background, pseudo-colored, and merged with SPOT RT camera software. Immunofluorescence images were segmented into splenic compartments and the number of pixels specific for Lm staining or fluorescent beads was measured and expressed as the percentage of pixels in each compartment (see Supplemental Data for details).

Pertussis Toxin and Clodronate Liposome Treatment

PTx was purchased from Sigma (St. Louis, MO). Mice were injected with 500 ng of PTx i.p. 1 day prior to infection (10^7 for 0.5 hr and 10^5 for 24 hr) and Lm tissue distribution was assessed by immunofluorescence at 0.5 and 24 hr later. In other experiments, the survival of PTx-treated mice after Lm infection with 10^3 CFU of EGD (LD_{50} ~2×10^3 in BALB/C mice) was determined. In 2P experiments, mice were given 500 ng PTx i.p. 1 day before to the transfer of fluorescently labeled Lm-specific and polyclonal T cells. T cells were allowed to home for several hours and then mice were infected by an i.v. injection of Lm (10^4 for EGD or 10^5 GFP-Lm). Approximately 9 hr later, spleen explants were cut and imaged with 2P microscopy and T cell behaviors (velocity and clustering) analyzed. In some experiments, PTx was administered 8–9 hr after infection to allow Lm time to enter the PALS. T cells were adoptively transferred 1–2 hr later and T cell behaviors analyzed with 2P microscopy for changes in motility and clustering beginning at ~2 hr after T cell transfer.

For depletion of phagocytes, clodronate liposome suspensions were prepared as described previously (Calderon et al., 2006; van Rooijen and van Kesteren-Hendrikx, 2003). Mice were given 200 μl of clodronate liposome suspension i.v. 2 or 6 days before infection. The depletion of macrophages and dendritic cells was assessed on day 2 and day 6 by staining sections for MARCO, MOMA-1, CD11b, and CD11c. Spleens were examined by immunofluorescence microscopy 24 hr after infection to quantify the amount of Lm in the MZ, RP, and PALS regions. Similar depletion and recovery experiments were preformed with the CD11c-DTR system of Jung et al. (Jung et al., 2002; Probst et al., 2005).

Two-Photon Microscopy

$CD8^+$ T cells were purified by negative selection with magnetic beads (Miltenyi Biotec) from BALB/cJ or WP11.12 mice (Mercado et al., 2000), then labeled for 30 min at 37°C with 20–50 μM CMAC, 10 μM CFSE, or 10 μM CMTMR (Invitrogen). T cells (5×10^5–7×10^6) were resuspended in 200 μl of PBS, adoptively transferred by tail vein injection and allowed to home for several hours before mice were infected with 10^5 EGD Lm. In some experiments, we infected mice with 10^6 GFP-expressing Lm to localize bacteria and T cell clusters in 3D space. Explanted spleens were secured to coverslips with a thin film of VetBond (3M). To image the WP, spleens were cut longitudinally with a vibratome (Pelco). Spleen sections were placed in a flow chamber and maintained at 37°C by perfusion with warm, high-glucose DMEM bubbled with a mixture of 95% O_2 and 5% CO_2. Time-lapse imaging was performed with a custom-built two-photon microscope, fitted with two Chameleon Ti:sapphire lasers (Coherent) and an Olympus XLUMPlanFI 20× objective (water immersed; numerical aperture, 0.95) and controlled and acquired with ImageWarp (A&B software). For imaging of GFP, the excitation wavelength was 890–915 nm; for CMTMR and CMAC, 780–800 nm was used. Signals from fluorescent dyes and GFP were separated by dichroic mirrors (490 nm, 515 nm, and 560 nm). To create time-lapse sequences, we typically scanned volumes of tissue 100 × 120 × 75 μm with 31 Z-steps of 2.5 μm each at 30–45 s intervals for up to 60 min.

CFSE T Cell Proliferation Assay

Purified $5–7 \times 10^6$ WP11.12 T cells were labeled with CFSE (5 μM) and transferred to recipient mice 2 hr before Lm infection (10^4). PTx-treated mice were given 500 ng of PTx i.p. 24 hr prior to infection with Lm (10^4 and 5×10^4). Beginning at 24 hr after infection, mice were given ampicillin (5 mg/ml in drinking water) to eliminate bacteria. On day 3 of infection, CFSE dilution was assessed by flow cytometry (2×10^6 cells) with Vβ8.1 to enrich for WP11.12 T cells in the analysis.

Data Analysis

Cells were detected based on fluorescence intensity and cell tracks obtained with Volocity (Improvision) or Imaris (Bitplane) software. Tracks greater than 3 min (≥7 time points) were included in the analysis. Cell velocities were reported as the median of instantaneous velocities in each cell track. Motility

coefficients ($\mu m^2\ min^{-1}$) were calculated for individual tracks by linear regression of displacement^2 versus time plots with T Cell Analysis (John Dempster, University of Strathclyde). Clusters were analyzed in five randomly selected time points with PicViewer (John Dempster, University of Strathclyde) as previously described (Zinselmeyer et al., 2005).

Statistical Analysis

Non-normally distributed data were presented as medians and compared with the Mann-Whitney U-test (two groups) or with an ANOVA followed by a suitable multiple comparison procedure (Dunn's or Dunnett's test).

SUPPLEMENTAL DATA

Supplemental Data include eight figures and seven movies and can be found with this article online at http://www.immunity.com/cgi/content/full/29/3/476/DC1/.

ACKNOWLEDGMENTS

The authors wish to acknowledge the following people: E. Unanue for many helpful discussions; R. Mebius for suggesting the clodronate-liposome experiments; J.A. Carrero, B. Calderon, and B. Ilian Strong for technical advice and useful suggestions; B. Nalibotski for help with custom acquisition scripts; J. Dempster for help with T cell motility analysis; E. Pamer for providing the WP11.12 transgenic mouse strain; N. Fortineau for providing pNF8 plasmid; and T. Nagata for generating the EGD GFP strain.

Received: February 13, 2008
Revised: May 20, 2008
Accepted: June 26, 2008
Published online: August 28, 2008

REFERENCES

Aichele, P., Zinke, J., Grode, L., Schwendener, R.A., Kaufmann, S.H., and Seiler, P. (2003). Macrophages of the splenic marginal zone are essential for trapping of blood-borne particulate antigen but dispensable for induction of specific T cell responses. J. Immunol. *171*, 1148–1155.

Angeli, V., and Randolph, G.J. (2006). Inflammation, lymphatic function, and dendritic cell migration. Lymphat. Res. Biol. *4*, 217–228.

Ato, M., Nakano, H., Kakiuchi, T., and Kaye, P.M. (2004). Localization of marginal zone macrophages is regulated by C-C chemokine ligands 21/19. J. Immunol. *173*, 4815–4820.

Belz, G.T., Shortman, K., Bevan, M.J., and Heath, W.R. (2005). CD8alpha+ dendritic cells selectively present MHC class I-restricted noncytolytic viral and intracellular bacterial antigens in vivo. J. Immunol. *175*, 196–200.

Bonasio, R., Scimone, M.L., Schaerli, P., Grabie, N., Lichtman, A.H., and von Andrian, U.H. (2006). Clonal deletion of thymocytes by circulating dendritic cells homing to the thymus. Nat. Immunol. *7*, 1092–1100.

Busch, D.H., Pilip, I.M., Vijh, S., and Pamer, E.G. (1998). Coordinate regulation of complex T cell populations responding to bacterial infection. Immunity *8*, 353–362.

Calderon, B., Suri, A., and Unanue, E.R. (2006). In CD4+ T-cell-induced diabetes, macrophages are the final effector cells that mediate islet beta-cell killing: Studies from an acute model. Am. J. Pathol. *169*, 2137–2147.

Cinamon, G., Zachariah, M.A., Lam, O.M., Foss, F.W., Jr., and Cyster, J.G. (2008). Follicular shuttling of marginal zone B cells facilitates antigen transport. Nat. Immunol. *9*, 54–62.

Conlan, J.W. (1996). Early pathogenesis of *Listeria monocytogenes* infection in the mouse spleen. J. Med. Microbiol. *44*, 295–302.

den Haan, J.M., Lehar, S.M., and Bevan, M.J. (2000). CD8(+) but not CD8(-) dendritic cells cross-prime cytotoxic T cells in vivo. J. Exp. Med. *192*, 1685–1696.

Dijkstra, C.D., Van Vliet, E., Dopp, E.A., van der Lelij, A.A., and Kraal, G. (1985). Marginal zone macrophages identified by a monoclonal antibody: characterization of immuno- and enzyme-histochemical properties and functional capacities. Immunology *55*, 23–30.

Dudziak, D., Kamphorst, A.O., Heidkamp, G.F., Buchholz, V.R., Trumpfheller, C., Yamazaki, S., Cheong, C., Liu, K., Lee, H.W., Park, C.G., et al. (2007). Differential antigen processing by dendritic cell subsets in vivo. Science *315*, 107–111.

Dufner, A., Duncan, G.S., Wakeham, A., Elford, A.R., Hall, H., Ohashi, P.S., and Mak, T.W. (2007). CARD6 is interferon-inducible but not involved in NOD signaling leading to NF-κ B activation. Mol. Cell. Biol. *28*, 1541–1552.

Elomaa, O., Kangas, M., Sahlberg, C., Tuukkanen, J., Sormunen, R., Liakka, A., Thesleff, I., Kraal, G., and Tryggvason, K. (1995). Cloning of a novel bacteria-binding receptor structurally related to scavenger receptors and expressed in a subset of macrophages. Cell *80*, 603–609.

Fortinea, N., Trieu-Cuot, P., Gaillot, O., Pellegrini, E., Berche, P., and Gaillard, J.L. (2000). Optimization of green fluorescent protein expression vectors for in vitro and in vivo detection of *Listeria monocytogenes*. Res. Microbiol. *151*, 353–360.

Germain, R.N., Miller, M.J., Dustin, M.L., and Nussenzweig, M.C. (2006). Dynamic imaging of the immune system: Progress, pitfalls and promise. Nat. Rev. Immunol. *6*, 497–507.

Glomski, I.J., Decatur, A.L., and Portnoy, D.A. (2003). *Listeria monocytogenes* mutants that fail to compartmentalize listerolysin O activity are cytotoxic, avirulent, and unable to evade host extracellular defenses. Infect. Immun. *71*, 6754–6765.

Huang, J.H., Cardenas-Navia, L.I., Caldwell, C.C., Plumb, T.J., Radu, C.G., Rocha, P.N., Wilder, T., Bromberg, J.S., Cronstein, B.N., Sitkovsky, M., et al. (2007). Requirements for T lymphocyte migration in explanted lymph nodes. J. Immunol. *178*, 7747–7755.

Itano, A.A., McSorley, S.J., Reinhardt, R.L., Ehst, B.D., Ingulli, E., Rudensky, A.Y., and Jenkins, M.K. (2003). Distinct dendritic cell populations sequentially present antigen to CD4 T cells and stimulate different aspects of cell-mediated immunity. Immunity *19*, 47–57.

Jung, S., Unutmaz, D., Wong, P., Sano, G., De los Santos, K., Sparwasser, T., Wu, S., Vuthoori, S., Ko, K., Zavala, F., et al. (2002). In vivo depletion of CD11c(+) dendritic cells abrogates priming of CD8(+) T cells by exogenous cell-associated antigens. Immunity *17*, 211–220.

Kamath, A.T., Pooley, J., O'Keeffe, M.A., Vremec, D., Zhan, Y., Lew, A.M., D'Amico, A., Wu, L., Tough, D.F., and Shortman, K. (2000). The development, maturation, and turnover rate of mouse spleen dendritic cell populations. J. Immunol. *165*, 6762–6770.

Khanna, K.M., McNamara, J.T., and Lefrancois, L. (2007). In situ imaging of the endogenous CD8 T cell response to infection. Science *318*, 116–120.

Kraal, G. (1992). Cells in the marginal zone of the spleen. Int. Rev. Cytol. *132*, 31–74.

Kraal, G., and Janse, M. (1986). Marginal metallophilic cells of the mouse spleen identified by a monoclonal antibody. Immunology *58*, 665–669.

Kursar, M., Höpken, U.E., Koch, M., Köhler, A., Lipp, M., Kaufmann, S.H., and Mittrücker, H.W. (2005). Differential requirements for the chemokine receptor CCR7 in T cell activation during *Listeria monocytogenes* infection. J. Exp. Med. *201*, 1447–1457.

Lauvau, G., Vijh, S., Kong, P., Horng, T., Kerksiek, K., Serbina, N., Tuma, R.A., and Pamer, E.G. (2001). Priming of memory but not effector CD8 T cells by a killed bacterial vaccine. Science *294*, 1735–1739.

Lindquist, R.L., Shakhar, G., Dudziak, D., Wardemann, H., Eisenreich, T., Dustin, M.L., and Nussenzweig, M.C. (2004). Visualizing dendritic cell networks in vivo. Nat. Immunol. *5*, 1243–1250.

Mackaness, G.B. (1962). Cellular resistance to infection. J. Exp. Med. *116*, 381–406.

Mariathasan, S., and Monack, D.M. (2007). Inflammasome adaptors and sensors: Intracellular regulators of infection and inflammation. Nat. Rev. Immunol. *7*, 31–40.

Mebius, R.E., and Kraal, G. (2005). Structure and function of the spleen. Nat. Rev. Immunol. *5*, 606–616.

Mercado, R., Vijh, S., Allen, S.E., Kerksiek, K., Pilip, I.M., and Pamer, E.G. (2000). Early programming of T cell populations responding to bacterial infection. J. Immunol. *165*, 6833–6839.

Metlay, J.P., Witmer-Pack, M.D., Agger, R., Crowley, M.T., Lawless, D., and Steinman, R.M. (1990). The distinct leukocyte integrins of mouse spleen dendritic cells as identified with new hamster monoclonal antibodies. J. Exp. Med. *171*, 1753–1771.

Miller, M.J., Wei, S.H., Parker, I., and Cahalan, M.D. (2002). Two-photon imaging of lymphocyte motility and antigen response in intact lymph node. Science *296*, 1869–1873.

Mitchell, J. (1973). Lymphocyte circulation in the spleen. Marginal zone bridging channels and their possible role in cell traffic. Immunology *24*, 93–107.

Muraille, E., Giannino, R., Guirnalda, P., Leiner, I., Jung, S., Pamer, E.G., and Lauvau, G. (2005). Distinct in vivo dendritic cell activation by live versus killed *Listeria monocytogenes*. Eur. J. Immunol. *35*, 1463–1471.

Neuenhahn, M., Kerksiek, K.M., Nauerth, M., Suhre, M.H., Schiemann, M., Gebhardt, F.E., Stemberger, C., Panthel, K., Schroder, S., Chakraborty, T., et al. (2006). CD8alpha+ dendritic cells are required for efficient entry of *Listeria monocytogenes* into the spleen. Immunity *25*, 619–630.

Odoardi, F., Kawakami, N., Li, Z., Cordiglieri, C., Streyl, K., Nosov, M., Klinkert, W.E., Ellwart, J.W., Bauer, J., Lassmann, H., et al. (2007). Instant effect of soluble antigen on effector T cells in peripheral immune organs during immunotherapy of autoimmune encephalomyelitis. Proc. Natl. Acad. Sci. USA *104*, 920–925.

Okada, T., and Cyster, J.G. (2007). CC chemokine receptor 7 contributes to Gi-dependent T cell motility in the lymph node. J. Immunol. *178*, 2973–2978.

Pamer, E.G. (2004). Immune responses to *Listeria monocytogenes*. Nat. Rev. Immunol. *4*, 812–823.

Park, J.H., Kim, Y.G., Shaw, M., Kanneganti, T.D., Fujimoto, Y., Fukase, K., Inohara, N., and Núñez, G. (2007). Nod1/RICK and TLR signaling regulate chemokine and antimicrobial innate immune responses in mesothelial cells. J. Immunol. *179*, 514–521.

Probst, H.C., Tschannen, K., Odermatt, B., Schwendener, R., Zinkernagel, R.M., and Van Den Broek, M. (2005). Histological analysis of CD11c-DTR/GFP mice after in vivo depletion of dendritic cells. Clin. Exp. Immunol. *141*, 398–404.

Serbina, N.V., Salazar-Mather, T.P., Biron, C.A., Kuziel, W.A., and Pamer, E.G. (2003). TNF/iNOS-producing dendritic cells mediate innate immune defense against bacterial infection. Immunity *19*, 59–70.

Shedlock, D.J., and Shen, H. (2003). Requirement for CD4 T cell help in generating functional CD8 T cell memory. Science *300*, 337–339.

Steinman, R.M., Pack, M., and Inaba, K. (1997). Dendritic cells in the T-cell areas of lymphoid organs. Immunol. Rev. *156*, 25–37.

Sun, J.C., and Bevan, M.J. (2003). Defective CD8 T cell memory following acute infection without CD4 T cell help. Science *300*, 339–342.

Unanue, E.R. (1997). Inter-relationship among macrophages, natural killer cells and neutrophils in early stages of *Listeria* resistance. Curr. Opin. Immunol. *9*, 35–43.

van Rooijen, N., and van Kesteren-Hendrikx, E. (2003). "In vivo" depletion of macrophages by liposome-mediated "suicide". Methods Enzymol. *373*, 3–16.

van Rooijen, N., Kors, N., and Kraal, G. (1989). Macrophage subset repopulation in the spleen: differential kinetics after liposome-mediated elimination. J. Leukoc. Biol. *45*, 97–104.

Wong, P., and Pamer, E.G. (2003). Feedback regulation of pathogen-specific T cell priming. Immunity *18*, 499–511.

Zinselmeyer, B.H., Dempster, J., Gurney, A.M., Wokosin, D., Miller, M., Ho, H., Millington, O.R., Smith, K.M., Rush, C.M., Parker, I., et al. (2005). In situ characterization of CD4(+) T cell behavior in mucosal and systemic lymphoid tissues during the induction of oral priming and tolerance. J. Exp. Med. *201*, 1815–1823.

Vaccine 26 (2008) 5165–5169

Contents lists available at ScienceDirect

Vaccine

journal homepage: www.elsevier.com/locate/vaccine

Chemokine receptor-mediated delivery of mycobacterial MPT51 protein efficiently induces antigen-specific T-cell responses

Masato Uchijima [a,*], Toshi Nagata [b], Yukio Koide [a]

[a] Department of Infectious Diseases, Hamamatsu University School of Medicine, 1-20-1 Handa-yama, Higashi-ku, Hamamatsu 431-3192, Japan
[b] Department of Health Science, Hamamatsu University School of Medicine, 1-20-1 Handa-yama, Higashi-ku, Hamamatsu 431-3192, Japan

ARTICLE INFO

Article history:
Available online 15 April 2008

Keywords:
DNA immunization
Chemokine
Tuberculosis

ABSTRACT

Here we evaluated the effects of immunization with a DNA vaccine encoding a fusion protein consisting of macrophage inflammatory protein-1α (MIP-1α) and MPT51 (a major secreted protein from *Mycobacterium tuberculosis*) on induction of specific $CD8^+$ T cells. The DNA vaccine encoding the fusion protein could induce significantly higher number of the antigen-specific $CD8^+$ T cells in mice than DNA vaccine encoding MPT51 alone. Also, splenocytes from mice immunized with the fusion DNA vaccine expressed higher level of IFN-γ mRNA and protein upon stimulation with an epitope peptide derived from MPT51 than those from mice immunized with a mixture of two DNA vaccines encoding either MPT51 or MIP-1α. These results suggest that DNA vaccine encoding MIP-1α-antigen fusion protein is able to be efficiently internalized into antigen-presenting cells via the chemokine receptor and induce higher level of antigen-specific $CD8^+$ T-cell responses.

1. Introduction

Mycobacterium tuberculosis, primary agent of tuberculosis (TB), is responsible for the three million deaths annually worldwide [1]. The only TB vaccine currently available is the attenuated *Mycobacterium bovis* strain bacillus Calmette-Guerin (BCG) which has been reported to have a variable protective efficiency [2]. The emergence of multi-drug-resistant strains of *M. tuberculosis* has given urgency to the need for novel agents and development of more effective vaccines.

Chemokines play an essential role in induction of inflammatory responses by trafficking of immune cells [3]. Chemokines bind to specific cell-surface receptors which are internalized after binding with ligands [4,5]. Chemokine receptors are differentially expressed on a variety of immune cells. Sentinel antigen-presenting cells (APCs), such as immature dendritic cells (DCs), express chemokine receptors such as CC chemokine receptor 5 (CCR5). CCR5 has been identified as the receptor for macrophage inflammatory protein-1α (MIP-1α), regulated on activation, normal T-cell expressed and secreted (RANTES), monocyte chemoattractant protein-1 (MCP-1), -2, -3, -4, and geotaxis [6]. CCR5 has been transported to early endosomes and subsequently recycled back to the cell surface or targeted for degradation [4]. Therefore, it should be possible to harness the receptor binding and internalization of chemokine to increase the immunogenecity of vaccines. MIP-1α binds to two kinds of receptors, CCR1 and CCR5, In contrast, RANTES or MCPs bind to more than three receptors. In this study, we focused on the CCR5 and its ligand, MIP-1α as a simple molecular and cellular targeting model. The efficacy of MIP-1α-antigen fusion was examined by using DNA vaccine against *M. tuberculosis*. Antigen-specific T-cell responses appeared to be significantly enhanced by genetic fusion of MIP-1α to MPT51, one of major protective antigens of *M. tuberculosis* [7].

2. Materials and methods

2.1. Fusion gene cloning and plasmid constructions

The eukaryotic expression vector, pCI (Promega, Madison, WI, USA) containing a cytomegalovirus (CMV) immediate-early promoter, chimeric intron, and SV40 late polyadenilation signal, was used for construction for DNA vaccines. Murine MIP-1α gene was cloned by reverse transcription (RT)-PCR from total RNA of DCs. MIP-1α gene was fused with MPT51 gene via 14-amino acids (GTNDAQAPKSLEGT) spacer sequence and cloned into the EcoRI/XbaI sites of pCI vector (pCI-MIP-1α-MPT51). A plasmid expressing MIP-1α alone was constructed for control experiments. MIP-1α-fused GFP expression plasmid, pCI-MIP-1α-GFP, was constructed by the same strategy.

* Corresponding author. Tel.: +81 53 435 2335; fax: +81 53 435 2335.
E-mail address: uchijima@hama-med.ac.jp (M. Uchijima).

0264-410X/$ – see front matter © 2008 Elsevier Ltd. All rights reserved.
doi:10.1016/j.vaccine.2008.03.059

2.2. Chemokine receptor binding assay

MIP-1α-fused GFP protein was prepared from the pCI-MIP-1α-GFP-transfected HEK293T cells. RAW264.7 cells, JAWS II cells or bone marrow-derrived DCs (BM-DCs) were incubated with the GFP fusion protein and phycoerythrin (PE)-labeled anti-CCR5 antibody (BD PharMingen, San Jose, CA, USA) for 30 min on ice and 15 min at room temperature. The samples were washed three times with phosphate-buffered saline (PBS) containing 1% fetal calf serum (FCS). Binding analysis was performed by using laser confocal microscopy (Olympus Fluoview, Tokyo, Japan).

2.3. Animals and immunization

BALB/c mice (between 8 and 10 weeks of age; Japan SLC, Hamamatsu, Japan) were maintained at the Institute for Experimental Animals, Hamamatsu University School of Medicine. All animal experiments were performed according to the Guideline for Animal Experimentation, Hamamatsu University School of Medicine.

For DNA immunization with Helios gene gun system (Bio-Rad Laboratories, Hercules, CA, USA), 0.5 mg of gold particles was coated with 1 μg of plasmid. Shaved skin of the abdomen was bombarded in vivo by two shots with the gene gun at a pressure of 400 psi. Each shot results in the delivery of 0.5 mg gold carrying 1 μg plasmid DNA on approximately 1 cm^2 of skin. Four BALB/c mice for each group were injected with 2 μg of plasmid DNA three times at 1-week intervals.

2.4. Analysis of $CD8^+$ T cells by tetramer complexes

An MPT51 24–32 peptide/H2-D^d tetramer complex was kindly supplied by the NIH Tetramer Facility. MHC/peptide tetramer assay was performed as described previously [8]. In brief, 3 days after the last immunization, spleen cells were prepared and stained with PE-conjugated MPT51 24–32 peptide/H2-D^d tetramer complexes and fluorescein isothiocyanate (FITC)-conjugated anti-CD8 (BD PharMingen) monoclonal antibody for 30 min at 4 °C. After washing, cells were resuspended in PBS containing 1% bovin serum albumin, and then analyzed on an EPICS XL digital flow cytometer (Beckman Coulter, Miami, FL, USA).

2.5. Quantitatification of IFN-γ mRNA with RT-PCR

Two weeks after the last immunization, spleen cells were prepared and plated at 1×10^7 cells/well in the presence of 1 μM of MPT51 24–32 peptide for 16 h. Total RNA was prepared by using ISOGEN (Nippon gene, Tokyo, Japan), and then quantitative RT-PCR was performed as described previously [9]. The nucleotide sequences of primers used in this study are as follows:

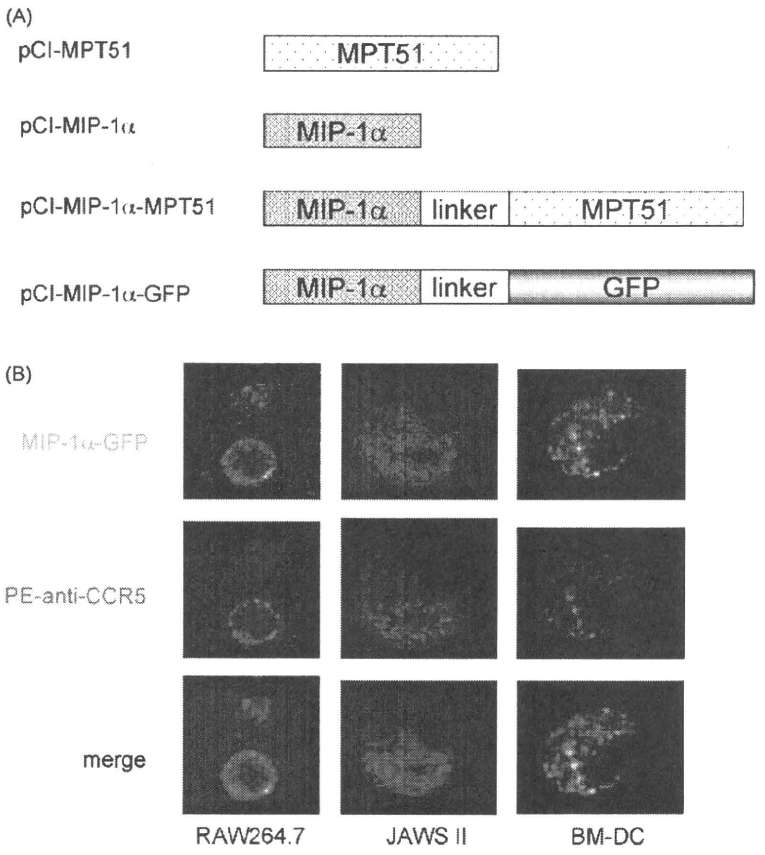

Fig. 1. (A) The schema of the gene products deduced from the expression vector plasmids prepared in this study. Mouse MIP-1α gene was cloned by RT-PCR from total RNA of dendritic cells. MIP-1α gene was fused with MPT51 gene via 14-amino acids spacer sequence (linker) and cloned into pCI vector. (B) Chemokine receptor binding assay. MIP-1α-fused GFP protein was prepared from the pCI-MIP-1α-GFP-transfected HEK293T cells. RAW264.7 cells, JAWS II cells, or BM-DCs were incubated with the GFP fusion protein and PE-labeled anti-CCR5 antibody for 30 min on ice and 15 min at room temperature. Binding analysis was performed by using laser confocal microscopy. (For interpretation of the references to color in the text, the reader is referred to the web version of the article.)

- IFN-γ:
  - 5′-TCTGAGACAATAAACGCTAC-3′ (forward);
  - 5′-GAATCAGCAGCGACTCCTTT-3′ (reverse).
- G3PDH:
  - 5′-ACCACAGTCCAT CCATCAC-3′ (forward);
  - 5′-TCCACCACCCTGTTGCTGTA-3′ (reverse).

2.6. Enzyme-linked immunosorbent assay (ELISA) of IFN-γ

Spleen cells were prepared from the immunized mice and plated in 96-well plates at 1×10^6 cells/well. Cells were stimulated with 1 μM of MPT51 24–32 peptide for 3 days. Concentration of IFN-γ in the culture supernatants was determined by a sandwich ELISA as described previously [10]. Data from multiple experiments were expressed in mean ± S.D. Statistical analyses were performed by using StatView-J 5.0 statistics program (SAS Institute Inc., Cary, NC, USA).

3. Results

3.1. Receptor binding and internalization of MIP-1α fusion protein

To investigate receptor binding and internalization of chemokine fusion protein, we constructed a MIP-1α-GFP expression plasmid (Fig. 1A). HEK293T cells were transiently transfected with pCI-MIP-1α-GFP plasmid and the cell lysates were used for receptor binding assay by using confocal microscopy. Most of the MIP-1α-GFP fusion proteins localized on the surface of murine macrophage-like RAW264.7 cells (Fig. 1B, left). Co-staining of the cells with PE-labeled ant-CCR5 antibody showed co-localization of the MIP-1α-GFP protein and CCR5. In contrast, the MIP-1α-GFP proteins readily localized in the cytoplasm of JAWS II, a murine dendritic cell line, in the same experimental condition (Fig. 1B, center). CCR5 co-localized with the GFP-fused MIP-1α in the cytoplasm, which was shown in yellow. Similar results were obtained when BM-DCs were incubated with the MIP-1α-GFP protein (Fig. 1B, right). Taken together, these data suggested that MIP-1α fusion protein is capable of binding to CCR5 and is efficiently internalized especially into DCs.

3.2. Induction of MPT51-specific CD8⁺ T cells after immunization with fusion DNA vaccine

To construct a DNA vaccine against TB, we used MPT51, a major secreted protein of *M. tuberculosis*, since we demonstrated that the MPT51 could induce T-cell-mediated immune responses and protective immunity upon challenge with *M. tuberculosis* [7]. In order to evaluate the effect of immunization with MIP-1α-fused DNA vaccine, the epitope-specific CTL responses were monitored by quantitating MHC/peptide tetramer binding to CD8⁺ T cells following DNA immunization. A representative experiment is shown in Fig. 2. The antigen-specific CD8⁺ T cells were higher in number in spleen cells of mice immunized with the fusion DNA vaccine as compared to those of mice immunized with DNA vaccine encoding MPT51 alone or combination with the MIP-1α expression plasmid. These experiments demonstrate that MIP-1α fusion DNA vaccine efficiently induces antigen-specific CD8⁺ T cells.

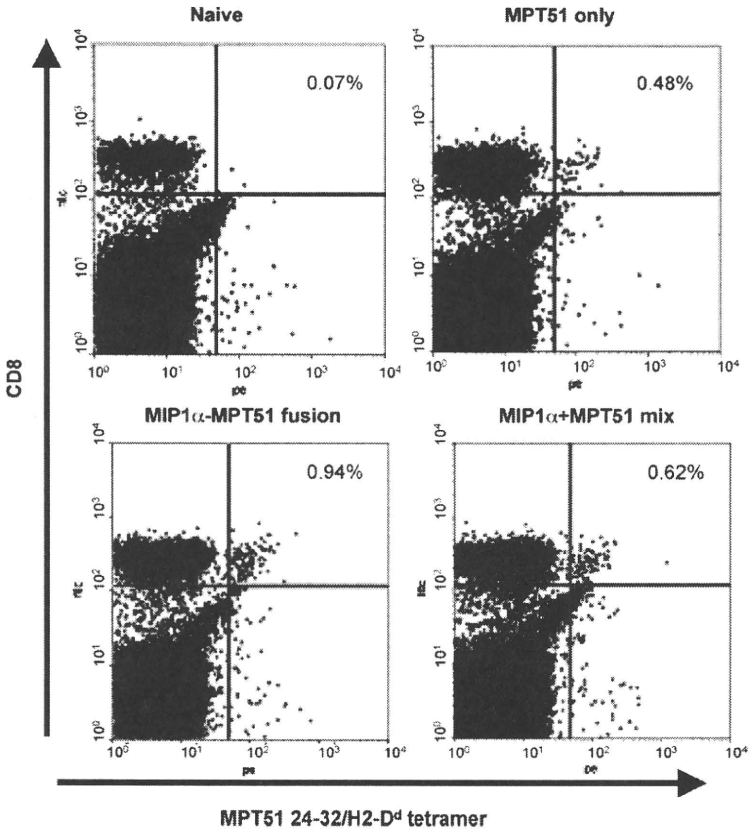

Fig. 2. Detection of MPT51-specific CD8⁺ T cells with MPT51 24–32/H2-D^d tetramer. Naïve and immune splenocytes were stained with PE-conjugated MPT51 24–32/H2-D^d tetramer complexes and FITC-conjugated anti-CD8 antibodies for 30 min at 4 °C. Stained cells were analyzed by a digital flow cytometer. Similar results were obtained in three independent experiments.

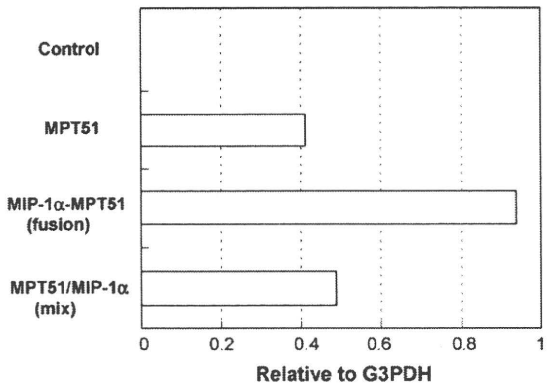

Fig. 3. IFN-γ mRNA expression of immune splenocytes in the presence of MPT51 peptide. Splenocytes were prepared 2 weeks after the last immunization and incubated with MPT51 peptide for 16 h. After preparation of total RNA, quantitative RT-PCR analysis was performed. Expression levels of mRNAs are shown relative to that of G3PDH mRNA. Similar results were obtained in three independent experiments.

3.3. Induction of the epitope-specific IFN-γ expression by spleen cells

We next examined the ability of antigen-specific IFN-γ mRNA expression in the DNA vaccine-immunized spleen cells. Two weeks after the last immunization, spleen cells from immunized mice were stimulated with MPT51 24–32 peptide, $CD8^+$ T-cell epitope derived from MPT51, for 16 h and the IFN-γ mRNA expression level was determined by real-time quantitative RT-PCR. Amounts of antigen-specific IFN-γ mRNA considerably increased in spleen cells from the fusion DNA vaccine-immunized mice as compared with those of pCI-MPT51- and pCI-MPT51 + pCI-MIP-1α-immunized mice (Fig. 3). Furthermore, we evaluated the production of IFN-γ by spleen cells of immunized mice after 3 days in vitro stimulation with MPT51 24–32 peptide employing ELISA. As shown in Fig. 4, spleen cells of mice immunized with the fusion DNA vaccine produced the highest level of IFN-γ protein in response to MPT51 24–32 peptide among these three DNA vaccination patterns consistent with the mRNA induction data (Fig. 3). A plasmid encoding MIP-1α showed adjuvant effect to some extent.

4. Discussion

The potency of vaccine presumably relies on the ability to recruit APCs and deliver antigens to them, leading to efficient antigen presentation to specific T cells. DCs are crucial in the activation of naïve T cells and induction of T cell-dependent immune responses. For this reason, experimental modification of vaccines, in particular genetic antigen delivery, has attracted much interest. Immature DCs, which are known as sentinel APCs, preferentially express CCR1, CCR2, CCR5, and CCR6 [11,12]. It has been reported that CCR1 or CCR5 internalizes into cells after ligand binding and recycles [4,5]. CCR5 also serves as a co-receptor for the entry of M-tropic human immunodeficiency into cells. Binding of viral gp120 to CCR5 reads to viral entry into the cells [13]. Therefore, it is possible to apply this phenomenon to vaccination. In this study, we evaluated the genetic fusion of MIP-1α to MPT51 to facilitate uptake and processing antigens, and to enhance DNA vaccine efficacy.

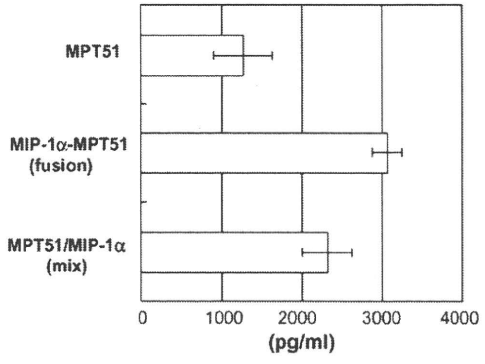

Fig. 4. IFN-γ production from immune splenocytes in response to MPT51 peptide stimulation. Immune spleen cells were cultured for 3 days at 1×10^7 ml^{-1} in the presence of MPT51 peptide. Concentration of IFN-γ in the culture supernatants was determined by ELISA. Results of four mice for each group are presented as mean ± S.D. Similar results were obtained in three independent experiments.

We here demonstrated that MIP-1α-GFP protein was quickly internalized and found in the cytosol, co-localized with CCR5 when a murine DC line, JAWS II cells or BM-DCs were incubated at room temperature (Fig. 1B). These data suggested that the fusion proteins not only retained its chemokine receptor binding properties of their nonfused chemokine counterparts, but also were efficiently internalized to the cytoplasm in immature DCs despite being linked to a relatively large antigen. The fate of the internalized MIP-1α fusion protein during receptor internalization remains unknown. Biragyn and his colleagues reported that MIP-3α fused melanoma-associated antigen are internalized via CCR6 to early/late endosomal and lysosomal compartment through a clathrin-dependent process and subsequently delivered to the cytosol for proteasomal processing, facilitating efficient cross-presentation to TAP-dependent MHC class I presentation pathway [14]. It is, therefore, possible that such cross-presentation is involved in the antigen-specific $CD8^+$ T cells induced with our MIP-1α-fused antigen.

Gene gun immunization is an efficient method for the administration of DNA vaccines [15]. Direct transfection of APCs or cross-presentation of exogenous antigen acquired from transfected nonimmune cells enables MHC class I-restricted activation of $CD8^+$ T cells [16,17]. Previously, we have reported that MPT51 possesses one $CD8^+$ T-cell epitope, p24–32, in BALB/c mice [18]. Therefore, we are able to examine the efficacy of MIP-1α-MPT51 DNA vaccine in inducing $CD8^+$ T cells using the epitope peptide. Using MPT51 24–32 peptide/H2-D^d tetramer, we demonstrated that gene gun immunizations into the skin of mice with plasmid DNA encoding MIP-1α-MPT51 protein induced high level of the epitope-specific $CD8^+$ T cells (Fig. 2). The efficient uptake of antigens by APCs may be particularly important for DNA vaccine, which typically expresses low amounts of antigen that are largely restricted to the local site of inoculation [19,20]. We also demonstrated that spleen cells from BALB/c mice immunized with DNA vaccine encoding MIP-1α-MPT51 secreted more IFN-γ in response to MPT51 24–32 peptide than those immunized with a DNA vaccine encoding MPT51 or with a mixture of two DNA vaccine encoding either MPT51 or MIP-1α. Several reports showed that co-immunization with DNA vaccines encoding antigens and chemokines enhanced the efficacy of vaccine by recruiting DCs to the inoculation sites [21]. In our hands, immunization with a mixture of pCI-MPT51 and pCI-MIP-1α also enhanced T-cell response although this activity was less than that induced by pCI-MIP-1α-MPT51 DNA vaccination. Furthermore, we also confirmed the effect of MIP-1α-MPT51 fusion protein vaccine. Mice immunized with MIP-1α-MPT51 fusion protein produced high level of MPT51-specific IFN-γ in response to MPT51 24–32 peptide (data not shown). This vaccine did not require the use of any additional adjuvants. In contrast, no antigen-specific IFN-γ production was induced in mice immunized with the mutant protein. Our data indicate that genetic fusion of chemokine to the antigen is more effective in terms of induction of T-cell responses than co-immunization methods.

In summary, our data suggest that MIP-1α-antigen fusion proteins encoded by DNA vaccine vector are efficiently internalized into APCs and induce higher level of antigen-specific T-cell responses. The immunization strategies shown here would be applicable to not only DNA vaccine but also to pre-monitoring the design of protein vaccination for induction of CTL.

Acknowledgements

We are grateful to Kiyoshi Shibata (Hamamatsu Univ. Sch. Med.) for excellent technical assistance. This work was supported by a grant-in-aid for scientific research and a grant-in-aid for centers of excellence (CoE) research program from the Ministry of Education, Culture, Sports, Science and Technology of Japan.

References

[1] Dyec C, Scheele S, Dolin P, Psthania V, Raviglione MC. Global burden of tuberculosis: estimated incidence, prevalence, and mortality by country. JAMA 1999;282:677–86.
[2] Colditz GA, Brewer TF, Berkey CS, Wilson ME, Burdick E, Fineberg HV, et al. Efficacy of BCG vaccine in the prevention of tuberculosis. JAMA 1994;271:698–702.
[3] Rollins BJ. Chemokines. Blood 1997;90:909–28.
[4] Mueller A, Kelly E, Strange PG. Pathways for internalization and recycling of the chemokine receptor CCR5. Blood 2002;99:785–91.
[5] Richardson RM, Pridgen BC, Haribabu B, Snyderman R. Regulation of the human chemokine receptor CCR1: cross-regulation by CXCR1 and CXCR2. J Biol Chem 2000;275:9201–8.
[6] Blanpain C, Migeotte I, Lee B, Vakili J, Dranz BJ, Govaerts C, et al. CCR5 binds multiple CC-chemokines: MCP-3 acts as a natural antagonist. Blood 1999;94:1899–905.
[7] Miki K, Nagata T, Tanaka T, Kim YH, Uchijima M, Ohara N, et al. Induction of protective cellular immunity against *Mycobacterium tuberculosis* by recombinant attenuated self-destructing *Listeria monocytogenes* strains harboring eukaryotic expression plasmids for antigen 85 complex and MPB/MPT51. Infect Immun 2004;72(4):2014–21.
[8] Aoshi T, Suzuki M, Uchijima M, Nagata T, Koide Y. Expression mapping using a retroviral vector for $CD8^+$ T cell epitopes: definition of a *Mycobacterium tuberculosis* peptide presented by $H2\text{-}D^d$. J Immunol Meth 2005;298:21–34.
[9] Uchijima M, Nagata T, Aoshi T, Koide Y. IFN-γ overcomes low responsiveness of myeloid dendritic cells to CpG DNA. Immunol Cell Biol 2005;83:92–5.
[10] Yoshida A, Koide Y, Uchijima M, Yoshida TO. Dissection of strain difference in acquired protective immunity against *Mycobacterium bovis* Calmette-Guerin bacillus (BCG). J Immunol 1995;155:2057–66.
[11] Sallusto F, Palermo B, Lenig D, Mietinnen M, Matikainen S, Julkunen I, et al. Distinct patterns and kinetics of chemokine production regulate dendritic cell function. Eur J Immunol 1999;29:1617–25.
[12] Dieu MC, Vanbervliet B, Vicari A, Bridon JM, Oldham E, Ait-Yahia S, et al. Selective recruitment of immature and mature dendritic cells by distinct chemokines expressed in different anatomic sites. J Exp Med 1998;188:373–86.
[13] Dragic T, Litwin V, Allaway GP, Martin SR, Huang Y, Nagashima KA, et al. HIV-1 entry into $CD4^+$ cells is mediated by the Chemokine receptor CC-CKR-5. Nature 1996;381:667–73.
[14] Schiavo R, Baatar D, Okuhanud P, Indig FE, Restifo N, Taub D, et al. Chemokine receptor targeting efficiently directs antigens to MHC class I pathways and elicits antigen-specific $CD8^+$ T-cell responses. Blood 2006;107:4597–605.
[15] Yoshida A, Nagata T, Uchijima M, Koide Y. Advantage of gene gun-mediated over intramuscular inoculation of plasmid DNA vaccine in reproducible induction of specific immune responses. Vaccine 2000;18:1725–9.
[16] Heath WR, Carbone FR. Cross-presentation in viral immunity and self-tolerance. Nat Rev Immunol 2001;1:126–34.
[17] Ulmer JB, Otten GR. Priming of CTL responses by DNA vaccines: direct transfection of antigen presenting cells versus cross-priming. Dev Biol (Basel) 2000; 104:9–14.
[18] Suzuki M, Aoshi T, Nagata T, Koide Y. Identification of murine $H2\text{-}D^d$- and $H2\text{-}A^b$-restricted T-cell epitopes on a novel protective antigen, MPT51, of *Mycobacterium tuberculosis*. Infect Immun 2004;72:3829–37.
[19] Casares S, Inaba K, Brumeanu TD, Steinman RM, Bona CA. Antigen presentation by dendritic cells after immunization with DNA encoding a major histocompatibility complex class II-restricted viral epitope. J Exp Med 1997;186: 1481–6.
[20] Barouch DH, Truitt DM, Letvin NL. Expression kinetics of the interleukin-2/immunoglobulin (IL-2/Ig) plasmid cytokine adjuvant. Vaccine 2004;22: 3092–7.
[21] Kutzler MA, Weiner DB. Developing DNA vaccines that call to dendritic cells. J Clin Invest 2004;114:1241–4.

Vaccine 26 (2008) 5123–5127

Contents lists available at ScienceDirect

Vaccine

journal homepage: www.elsevier.com/locate/vaccine

In vivo hierarchy of individual T-cell epitope-specific helper T-cell subset against an intracellular bacterium

Toshi Nagata [a,*], Taiki Aoshi [b], Masato Uchijima [b], Yukio Koide [b]

[a] Department of Health Science, Hamamatsu University School of Medicine, 1-20-1 Higashi-ku, Handa-yama, Hamamatsu 431-3192, Japan
[b] Department of Infectious Diseases, Hamamatsu University School of Medicine, 1-20-1 Higashi-ku, Handa-yama, Hamamatsu 431-3192, Japan

ARTICLE INFO

Article history:
Available online 14 April 2008

Keywords:
DNA immunization
Th epitope
Listeria monocytogenes

ABSTRACT

Cellular immunity is indispensable for efficient protection against intracellular bacterial infection. $CD4^+$ and $CD8^+$ T cells specific for a variety of antigenic peptides derived from particular bacteria are induced after the infection. T cells recognizing different antigenic peptides have been speculated to have different functions in terms of the protective immunity. We here induced individual $CD4^+$ T cells specific for each antigenic peptide derived from *Listeria monocytogenes* independently with DNA vaccines using gene gun bombardment and compared the $CD4^+$ T-cell populations for their ability on the specific protective immunity against lethal listerial challenge and analyzed their characteristics.

1. Introduction

Listeria monocytogenes is a facultative Gram-positive intracellular bacterium. Murine infection with *L. monocytogenes* is an excellent model system for studying cellular immunity against intracellular microorganisms [1]. For the protection against the microorganism, $CD4^+$ helper T-lymphocytes (Th), in addition to $CD8^+$ cytotoxic T-lymphocytes (CTL), which are specifically amplified at listerial infection, have been shown to play a critical role in the protective immunity against challenge by lethal dose of *L. monocytogenes* [2–5].

$CD4^+$ T-cell epitopes as well as $CD8^+$ T-cell epitopes, derived from *L. monocytogenes* have been identified so far. Especially, T-cell epitopes derived from two critical virulent factors of *L. monocytogenes*, listeriolysin O (LLO) and p60 protein have been intensively studied. LLO is a sulfhydryl-activated pore-forming exotoxin. It allows the bacterium to escape from the phagosome and to replicate in the cytoplasm [1]. LLO 215–226 was first identified as a dominant $CD4^+$ Th epitope restricted to H2-E^k molecule [6,7]. p60 protein is a murein hydrolase and has been shown to be involved in the invasion of mammalian cells [1]. Following LLO 215–226 peptide, p60 301–312 was then reported as an H2-A^d-restricted $CD4^+$ Th epitope [8]. Further, Geginat et al. [9] reported several T-cell epitopes of LLO and p60 protein in BALB/c and C57BL/6 mice using an approach for the direct ex vivo identification and characterization of T-cell epitopes based on the screening of peptide spot libraries with ex vivo isolated spleen cells in a highly sensitive enzyme-linked immunospot (ELISPOT) assay. They found in their system, four $CD8^+$ T-cell epitopes and six $CD4^+$ T-cell epitopes in BALB/c mice and two $CD8^+$ T-cell epitopes and five $CD4^+$ T-cell epitopes in C57BL/6 mice including previously identified ones [9].

In our previous works, we have investigated individual T-cell epitope-specific T-cell responses against *L. monocytogenes* using minigene DNA vaccine system [10–12]. For $CD8^+$ T-cell epitope-specific responses, we showed that interaction between T cells against dominant and subdominant epitopes does not operate in the generation of the hierarchy among individual $CD8^+$ T-cell epitopes with minigene DNA vaccination [11]. For $CD4^+$ T-cell epitope-specific responses, we have reported that LLO 215–226-specific T-cell response evoked by DNA vaccination was capable of inducing protective immunity against lethal listerial challenge in C3H mice [13].

Here, we compared four different H2-A^d-, or H2-E^d-restricted $CD4^+$ T-cell epitope-specific responses in terms of the protective immunity in BALB/c mice by immunization of invariant chain (Ii) cDNA whose major histocompatibility complex (MHC) class II-associated Ii peptide (CLIP) region was replaced by the antigenic peptides. The antigenic peptide/CLIP-replaced Ii gene immunization would be an efficient method for presenting antigenic peptides of interest to Th in vivo [13–16]. Using this system, each individual epitope peptide has been expected to be expressed in similar amounts in vivo [11] and would be feasible for evaluation of each $CD4^+$ T-cell epitope peptide for induction of the specific T-cell

* Corresponding author. Tel.: +81 53 435 2332; fax: +81 53 435 2332.
E-mail address: tnagata@hama-med.ac.jp (T. Nagata).

0264-410X/$ – see front matter © 2008 Elsevier Ltd. All rights reserved.
doi:10.1016/j.vaccine.2008.03.061

responses including the protective ability against following listerial challenge.

2. Materials and methods

2.1. Animals

BALB/c mice (Japan SLC, Hamamatsu, Japan) were maintained in the Animal Facility of Hamamatsu University School of Medicine. Mice between 6 and 18 weeks of age were used for immunization. All animal experiments were performed according to the Guidelines for Animal Experimentation, Hamamatsu University School of Medicine.

2.2. Plasmid construction

pCI-mli p41-LLO215m, a DNA vaccine plasmid for LLO 215–226 (SQLIAKFGTAFK), has been reported previously [13]. DNA vaccine plasmids for LLO 189–200 (WNEKYAQAYPNV; pCI-mli p41-LLO 189m), p60 367–378 (SSASAIIAEAAQK; pCI-mli p41–p60 367m), and p60 301–312 (EAAKPAPAPSTN; pCI-mli p41–p60 301m) were constructed similarly (Fig. 1). In brief, double-stranded oligonucleotides coding for each T-cell epitope peptide replaced HindIII–NspI DNA fragment coding for CLIP region of murine Ii p41 molecule in pCI-mli p41 plasmid [13,15]. The oligonucleotides for T-cell epitopes derived from *L. monocytogenes* were codon-optimized to mouse. The nucleotide sequences of the resultant plasmids were confirmed by dideoxy sequencing, using ABI PRISM 310 Genetic Analyzer (Applied Biosystems, Foster City, CA, USA). During the cloning procedure, the DNA fragments were purified from agarose gels using GeneClean II kit (Bio 101, La Jolla, CA, USA). Large-scale purification of plasmids was conducted with Qiagen plasmid mega kit system (Qiagen, Valencia, CA, USA) and endotoxin was removed by Triton X-114 phase separation.

2.3. DNA immunization

For DNA immunization with Helios gene gun system (Bio-Rad Laboratories, Hercules, CA, USA), preparation of the cartridge of DNA-coated gold particle cartridge was followed to the manufacturer's instruction manual. Finally, 0.5 mg of gold particles was coated with 1 μg of plasmid DNA and the injection was carried out with 0.5 mg gold per shot twice. Mice were injected with 2 μg of plasmid DNA four times at 1-week intervals.

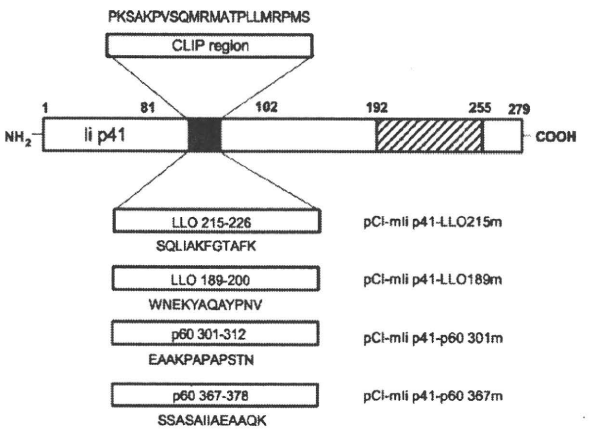

Fig. 1. The schema of murine Ii p41 molecule whose CLIP is replaced by LLO 215–226, LLO 189–200, p60 367–378, or p60 301–312 deduced from the cDNA construct (pmli p41-LLO215 m, pmli p41-LLO189 m, pmli p41–p60 367 m, or pmli p41–p60 301 m, respectively). The deduced amino acid sequences of the replaced CLIP region and the Th-epitope peptides are shown. Amino acid numbers of each domain of murine Ii p41 molecule are also shown.

2.4. Lymphocyte proliferation assay

Spleen cells (5×10^5 per well) from the immunized mice were maintained with RPMI-1640 medium supplemented with 10% fetal bovine serum (FBS) at 37 °C in a humidified 5% CO_2 atmosphere. They were incubated for 48 h at 37 °C in 96-well round-bottom tissue culture plates in the presence or absence of 1 μM of individual Th-epitope peptide. After 48 h in culture, de novo DNA synthesis was assessed by adding 0.5 μCi per well [methyl-^{3}H] thymidine (10 Ci mmol^{-1}; ICN Biochemicals, Irvine, CA, USA) for the last 12 h of culture. Triplicate cultures were harvested onto glass fiber filters, and the [methyl-^{3}H] thymidine incorporation was determined by counting the radioactivity (cpm) using liquid scintillation counter.

2.5. Bacterial infection

L. monocytogenes EGD strain was kept virulent by in vivo passage. For the inoculation, a seed of *L. monocytogenes* was cultured overnight in trypticase soy broth (BBL, Sparks, MD, USA) at 37 °C in a bacterial shaker and suitably diluted with phosphate-buffered saline. The exact infection dose was assessed retrospectively by plating. Mice were immunized four times with DNA vaccine plasmids as described above. One month later, the mice were challenged with 2×10^4 CFU of *L. monocytogenes* by intravenous injection. Bacterial numbers of the spleens were determined 72 h after the challenge infection by plating 10-fold dilutions of tissue homogenates on trypticase soy agar plates (BBL).

2.6. Cytokine assay for spleen cells from immunized mice

One month after the last immunization, spleen cells were harvested from the immunized mice. Recovered cells were plated in 24-well plates at 2×10^6 cells per well in the presence or absence of 1 μM of individual T-cell epitope peptide for 5 days. Concentration of cytokines (interferon (IFN)-γ, tumor necrosis factor (TNF)-α, interleukin (IL)-5, IL-4, IL-2) in culture supernatants was determined by cytometric bead assay (CBA). Fifty micro-liter of culture supernatants were assayed for these cytokines using mouse Th1/Th2 cytokine CBA kit (BD Biosciences Pharmingen, San Diego, CA, USA) according to the manufacturer's instruction.

2.7. Statistics

Data from multiple experiments were expressed as the means ± S.E. Statistical analyses were performed by using StatView-J 5.0 statistics program (Abacus Concepts, Berkeley, CA, USA). Data were analyzed with one factor-analysis of variance followed by the Fisher's protected least significant difference test.

3. Results

3.1. Proliferative responses of spleen cells of mice immunized with expression plasmids for Th epitopes

In order to examine CD4$^+$ T-cell responses against four different Th epitopes of *L. monocytogenes* in BALB/c mice, we constructed four DNA vaccine plasmids for in vivo antigen presentation of LLO 215–226, LLO 189–200, p60 367–378, and p60 301–312 (Fig. 1). The DNA vaccine constructs are expression plasmids for recombinant murine Ii cDNA whose CLIP region were replaced by an oligonucleotide encoding CD4$^+$ T-cell epitope peptide [13,15]. The plasmid DNAs were injected by gene gun bombardment into BALB/c mice

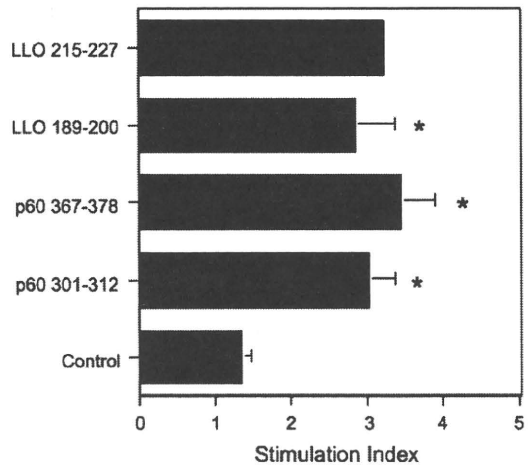

Fig. 2. Individual Th-epitope-specific proliferative responses of spleen cells from mice immunized with Th-epitope expression plasmids. BALB/c mice were immunized with each plasmid by using gene gun four times at 1-week intervals. Spleen cells from the immunized mice were harvested 1 month after the last immunization and cultured in vitro (5×10^5 per well) in the presence or absence of 1 μM of each Th-epitope peptide for 2 days and pulsed with 0.5 μCi of [methyl-^{3}H] thymidine for last 12 h. Results of control wild-type li p41 expression plasmid-immunized mice are also shown as a control. The means ± S.E. of stimulation index (cpm in the presence of the peptide divided by cpm in the absence of the peptide) of three mice per group are shown except for two mice for LLO 215–227 group. Asterisks indicate statistical significance ($p < 0.05$) compared with the value of control mice.

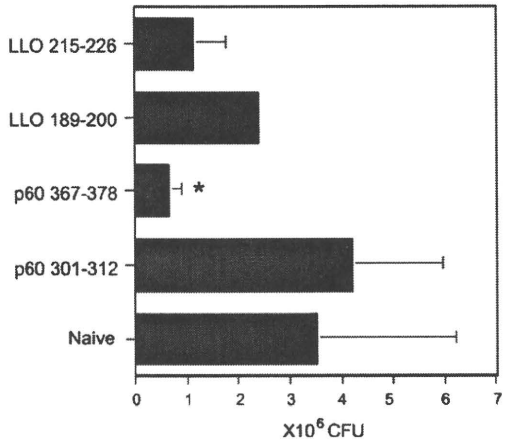

Fig. 3. Evaluation of protective immunity induced by immunization with Th-epitope expression plasmids. Mice were immunized with each Th-epitope expression plasmid four times at 1-week intervals. One month after the last immunization, the immunized mice were challenged i.v. with 2 × 103 CFU of *L. monocytogenes*. Bacterial numbers in the spleens were determined 72 h after the challenge infection by plating 10-fold dilutions of tissue homogenates on trypticase soy agar plates. Results of naive mice are also shown as a control (Naive). Results are expressed as the mean ± S.E. for three to four mice for each group except for two mice for LLO 189–200 group. Asterisk indicates statistical significance ($p < 0.05$) compared with the value of mice immunized with p60 301–312 DNA vaccine.

as shown in Materials and methods section. We chose the immunization method as it was a very reliable and reproducible method from our previous experience [17].

First, we performed lymphocyte proliferation assay one month after the last immunization. As shown in Fig. 2, immunization with each Th-epitope peptide expression plasmid induced individual peptide-specific proliferative responses of the spleen cells. The stimulation indexes were similar for four T-cell epitope peptides. These results indicated that the DNA vaccination successfully induced individual epitope-specific T-cell responses.

3.2. Induction of protective immunity against listerial infection after immunization with Th epitope expression plasmids

In order to examine whether the immunity evoked by immunization with each Th-epitope peptide expression plasmid is associated with an increased resistance to infection of virulent *L. monocytogenes*, the in vivo protection experiment was carried out. Seventy-two hours after listerial challenge, mice were sacrificed and CFU from the spleens were counted. As shown in Fig. 3, bacterial number in spleens of mice immunized with plasmids for p60 367–378 and LLO 215–226 tended to be reduced compared with that of naïve mice. On the contrary, bacterial number in spleens of mice immunized with plasmids for p60 301–312 and LLO 189–200 tended to be similar with that of naïve mice. Immunization with plasmid for p60 301–312 even increased the bacterial number in spleens compared with that of naive mice.

3.3. Cytokine production from spleen cells of mice immunized with expression plasmids for individual Th epitopes

We are interested in what caused different protective effects by immunization with these different Th-epitope peptide expression plasmids. One of the reasons may be cytokine profiles produced by specific Th. We therefore analyzed cytokine profiles in the supernatants of immune spleen cell culture after 5-day in vitro stimulation with individual Th-epitope peptides.

As shown in Fig. 4, spleen cells from mice immunized with plasmids for LLO 215–226 and p60 367–378 tended to express TNF-α and IFN-γ after the Th-epitope peptide stimulation. Whereas, immune spleen cells with plasmids for LLO 189–200 and p60 301–312 tended to withdraw the expression of IFN-γ, although these tendencies were rather moderate.

4. Discussion

Following infection from a variety of pathogenic microorganisms, specific CD4$^+$ and CD8$^+$ T-cell responses are induced against various antigens of the microorganisms. CD8$^+$ T-cell responses are evoked mainly by microorganisms located in the cytoplasm

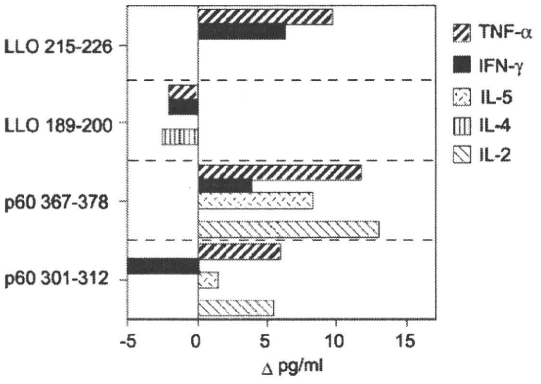

Fig. 4. Cytokine productions by spleen cells from Th-epitope expression plasmid-immunized mice. The spleen cells of mice immunized with each Th-epitope expression plasmid were harvested 1 month after the last immunization and cultured in vitro in the presence or absence of 1 μM of each Th-epitope peptide for 5 days, and the culture supernatants were analyzed by CBA. The values represent the means of Δpg/ml (the value in the presence of the peptide minus the value in the absence of the peptide) of two mice per each group.

of host cells, e.g., in the case of infection of viruses, as well as *L. monocytogenes*. $CD4^+$ T-cell responses are induced mainly by infection of extracellularly located microorganisms or microorganisms located in the phagosome, e.g., in the case of infection of *Salmonella*, *Legionella*, and *Mycobacterium* spp. [18]. $CD4^+$ T-cell responses have been also shown to be induced by *L. monocytogenes* and play an important role in the protective immunity against listerial challenge. In murine *Listeria* infection model, $CD4^+$ T-cell responses have been studied. MHC class II gene-deficient mice were reported to be more sensitive to lethal listerial challenge compared with their control heterozygous littermates [19]. Geginat et al. [8] reported that adoptive transfer of p60 301–312-specific IFN-γ-producing $CD4^+$ T-cell line into BALB/c mice induced protective immunity against lethal listerial challenge, suggesting that $CD4^+$ T cells are positively involved in protective immunity. On the contrary, Kursar et al. [20] reported that depletion of $CD4^+$ T cells during immunization with nonviable *L. monocytogenes* enhanced $CD8^+$ T cell-mediated protection against listeriosis, suggesting involvement of regulatory T-cell population in failure of induction of protective immunity by nonviable *Listeria* vaccination.

There has been reported functional diversity of helper T cells [21]. Especially, so-called T helper 1 (Th1)/T helper 2 (Th2) dichotomy has been reported to be important for determining the following immunological outcome [22]. Th1-type $CD4^+$ T cells produce abundant IFN-γ, TNF-α, or IL-2. These cytokines were known to be involved mainly in cell-mediated immunity. Preexisting memory $CD4^+$ Th1, but not Th2 T-cell subset at the time of $CD8^+$ T-cell priming resulted in increased $CD8^+$ T-cell responses to bacterial and viral pathogens [23]. On the contrary, Th2-type $CD4^+$ T-cells produce IL-4, IL-5, or IL-10. These cytokines were known to be involved in humoral immunity. Induction of Th1 or Th2 $CD4^+$ T cells would be affected by many variable factors. They include, immunization method used, type of antigen-presenting cells and/or density of costimulatory molecules on the cells, factors evoking innate immunity such as adjuvants and infectious agents. Further, antigenic peptide dose may be critical for determining Th1/Th2 balance. Hosken et al. [24] investigated the relationship of antigenic peptide dose and Th1/Th2 selection using an in vitro system with naive T cells from ovalbumin-specific T-cell receptor transgenic mice. In the system, they showed that low peptide dose (0.01–0.04 μM) induced Th2 responses (dominant IL-4 production and less IFN-γ production) and high peptide dose (3.7–100 μM) induced Th1 responses (dominant IFN-γ production).

In addition to them, several reports suggested antigenic peptide affinity to MHC may also be involved in determining Th1/Th2 selection [25–27]. The peptides of higher affinity for a given MHC class II molecule elicited a shift towards the Th1 subset. In our work, exact affinity of peptides to MHC was not clear, but RANKPEP MHC-binding peptide prediction program (http://bio.dfci.harvard.edu/Tools/rankpep.html) predicted the affinity by calculating MHC-binding scores for each peptide. The scores for antigenic peptides studied here were as follows. LLO 215–226, 11.829 for H2-E^d; LLO 189–200, 7.104 for H2-A^d; p60 367–378, 11.261 for H2-A^d; p60 301–312, 11.44 for H2-A^d. The scores seemed not so different from each other except for LLO 189–200, whose score showed somewhat lower than those of other peptides. T-cell receptor affinity for the peptide-MHC and T-cell receptor repertoire (which may affect T-cell receptor Vβ chain usage) may also affect the Th1/Th2 selection.

In this study, we compared four $CD4^+$ T-cell epitope-specific T-cell responses against *L. monocytogenes* using gene gun DNA vaccine system. We used DNA vaccines of $CD4^+$ T-cell epitope peptide-Ii chain cDNA chimeric DNA constructs for that purpose as described in our previous work [13,15]. The results in this study showed that individual epitope-specific $CD4^+$ T-cell responses are different in terms of protective immunity and cytokine production profiles although the same DNA vaccination system was performed for each epitope-specific $CD4^+$ T cells. In results of the in vivo protection experiment, p60 367–378-specific and LLO 215–226-specific T-cells tended to have protective ability against listeriosis, but p60 301–312-specific and LLO 189–200-specific T cells did not (Fig. 3). Related with the result, p60 367–378 and LLO 215–226 peptides had tendency to induce IFN-γ production, whereas, p60 301–312 and LLO 189–200 peptides did not in the cytokine assay (Fig. 4). These apparent results suggest that the level of IFN-γ production may affect the protective ability of each peptide-specific T cells.

We tried to evaluate cytokine profiles of each T-cell epitope-specific T cells using CBA system, but the cytokine expression levels were rather moderate. This may be caused by several reasons. BALB/c mice may induce relatively low $CD4^+$ T-cell responses when compared with $CD8^+$ T-cell responses to LLO and p60 molecules of *L. monocytogenes* [9]. Further evaluation would be definitely necessary.

In conclusion, selection of $CD4^+$ T-cell epitopes would be critical for construction of multi-epitope vaccination. Minigene DNA vaccination would serve a feasible system for evaluation of each T-cell epitope for induction of protective immunity against various pathogens.

Acknowledgements

We thank Dr. M. Mitsuyama (Kyoto University, Japan) for generously providing the *L. monocytogenes* EGD strain. This work was supported by Grants-in-Aid for Scientific Research from the Japanese Society for the Promotion of Science [11670260 (T.N.), 13670268 (Y.K.)] and a Grant-in-Aid for Centers of Excellence (COE) research program from the Ministry of Education, Culture, Sports, Science and Technology of Japan.

References

[1] Pamer EG. Immune responses to *Listeria monocytogenes*. Nat Rev Immunol 2004;4:812–23.
[2] Kaufmann SHE, Hug E, Vath U, Muller I. Effective protection against *Listeria monocytogenes* and delayed-type hypersensitivity to listerial antigens depend on cooperation between specific L3T4⁺ and Lyt2⁺ T cells. Infect Immun 1985;48:263–6.
[3] Kaufmann SHE, Hug E, Vath U, De Libero G. Specific lysis of *Listeria monocytogenes*-infected macrophages by class II-restricted L3T4⁺ T cells. Eur J Immunol 1987;17:237–46.
[4] Magee DM, Wing EJ. Cloned L3T4⁺ T lymphocytes protect mice against *Listeria monocytogenes* by secreting IFN-γ. J Immunol 1988;141:3203–7.
[5] Rakhmilevich AL. Evidence for a significant role of $CD4^+$ T cells in adoptive immunity to *Listeria monocytogenes* in the liver. Immunology 1993;82:249–54.
[6] Safley SA, Jensen PE, Reay PA, Ziegler HK. Mechanisms of T cell epitope immunodominance analyzed in murine listeriosis. J Immunol 1995;155:4355–66.
[7] Ziegler HK, Safley SA, Hiltbold E. Definition of T cell epitopes of *Listeria monocytogenes* and regulation of antigen processing by the bacterial exotoxin listeriolysin-O (LLO). In: Humphreys RE, Pierce SK, editors. Antigen processing and presentation. San Diego: Academic Press; 1994. p. 295–307.
[8] Geginat G, Lalic M, Kretschmar M, Goebel W, Hof H, Palm D, et al. Th1 cells specific for a secreted protein of *Listeria monocytogenes* are protective in vivo. J Immunol 1998;160:6046–55.
[9] Geginat G, Schenk S, Skoberne M, Goebel W, Hof H. A novel approach of direct ex vivo epitope mapping identifies dominant and subdominant CD4 and CD8 T cell epitopes from *Listeria monocytogenes*. J Immunol 2001;166:1877–84.
[10] Uchijima M, Yoshida A, Nagata T, Koide Y. Optimization of codon usage of plasmid DNA vaccine is required for the effective MHC class I-restricted T cell responses against an intracellular bacterium. J Immunol 1998;161:5594–9.
[11] Yamada T, Uchiyama H, Nagata T, Uchijima M, Suda T, Chida K, et al. Protective cytotoxic T lymphocyte responses induced by DNA immunization against immunodominant and subdominant epitopes of *Listeria monocytogenes* are noncompetitive. Infect Immun 2001;69:3427–30.
[12] Nagata T, Aoshi T, Uchijima M, Suzuki M, Koide Y. Cytotoxic T-lymphocyte-, and helper T-lymphocyte-oriented DNA vaccination. DNA Cell Biol 2004;23(2):93–106.

[13] Nagata T, Aoshi T, Suzuki M, Uchijima M, Kim Y-H, Yang Z, et al. Induction of protective immunity to *Listeria monocytogenes* by immunization with plasmid DNA expressing a helper T-cell epitope that replaces the class II-associated invariant chain peptide of the invariant chain. Infect Immun 2002;70:2676–80.
[14] van Bergen J, Ossendorp F, Jordens R, Mommaas AM, Drijfhout J-W, Koning F. Get into the groove! Targeting antigens to MHC class II. Immunol Rev 1999;172:87–96.
[15] Nagata T, Higashi T, Aoshi T, Suzuki M, Uchijima T, Koide Y. Immunization with plasmid DNA encoding MHC class II binding peptide/CLIP-replaced invariant chain (Ii) induces specific helper T cells in vivo: the assessment of Ii p31 and p41 isoforms as vehicles for immunization. Vaccine 2001;20:105–14.
[16] van Tienhoven EAE, ten Brink CTB, van Bergen J, Koning F, van Eden W, Broeren CPM. Induction of antigen specific CD4+ T cell responses by invariant chain based DNA vaccines. Vaccine 2001;19:1515–9.
[17] Yoshida A, Nagata T, Uchijima M, Higashi T, Koide Y. Advantage of gene gun-mediated over intramuscular inoculation of plasmid DNA vaccine in reproducible induction of specific immune responses. Vaccine 2000;18:1725–9.
[18] Kaufmann SHE. Immunity to intracellular bacteria. In: Paul WE, editor. Fundamental immunology. 5th ed. Philadelphia: Lippincott Williams & Wilkins Publishers; 2003. p. 1229–61.
[19] Ladel CH, Inge EA, Arnoldi J, Kaufmann SHE. Studies with MHC-deficient knockout mice reveal impact of both MHC I- and MHC II-dependent T cell responses on *Listeria monocytogenes* infection. J Immunol 1994;153:3116–22.
[20] Kursar M, Köhler A, Kaufmann SHE, Mittrücker H-W. Depletion of CD4+ T cells during immunization with nonviable *Listeria monocytogenes* causes enhanced CD8+ T cell-mediated protection against listeriosis. J Immunol 2004;172:3167–72.
[21] Abbas AK, Murphy KM, Sher A. Functional diversity of helper T lymphocytes. Nature 1996;383:787–93.
[22] Constant SL, Bottomly K. Induction of Th1 and Th2 $CD4^+$ T cell responses: the alternative approaches. Annu Rev Immunol 1997;15:297–322.
[23] Krawczyk CM, Shen H, Pearce EJ. Memory CD4 T cells enhance primary CD8 T-cell responses. Infect Immun 2007;75:3556–60.
[24] Hosken NA, Shibuta K, Heath AW, Murphy KM, O'Garra A. The effect of antigen dose on $CD4^+$ T helper cell phenotype development in a T cell receptor-$\alpha\beta$-transgenic model. J Exp Med 1995;182:1579–84.
[25] Pfeffer C, Stein J, Southwood S, Ketelaar H, Sette A, Bottomly K. Altered peptide ligands can control CD4 T lymphocyte differentiation in vivo. J Exp Med 1995;181:1569–74.
[26] Murray JS. How the MHC selects Th1/Th2 immunity. Immunol Today 1998; 19(4):157–63.
[27] Creusot RJ, Thomsen LL, Tite JP, Chain BM. Local cooperation dominates over competition between $CD4^+$ T cells of different antigen/MHC specificity. J Immunol 2003;171:240–6.

Vaccine 26 (2008) 5095–5100

Contents lists available at ScienceDirect

Vaccine

journal homepage: www.elsevier.com/locate/vaccine

Intratracheal administration of third-generation lentivirus vector encoding MPT51 from *Mycobacterium tuberculosis* induces specific CD8+ T-cell responses in the lung

Dai Hashimoto[a], Toshi Nagata[b], Masato Uchijima[c], Shintaro Seto[c], Takafumi Suda[a], Kingo Chida[a], Hiroyuki Miyoshi[d], Hirotoshi Nakamura[a], Yukio Koide[c,*]

[a] *Department of Internal Medicine, Hamamatsu University School of Medicine, 1-20-1 Higashi-ku, Handa-yama, Hamamatsu 431-3192, Japan*
[b] *Department of Health Science, Hamamatsu University School of Medicine, 1-20-1 Higashi-ku, Handa-yama, Hamamatsu 431-3192, Japan*
[c] *Department of Infectious Diseases, Hamamatsu University School of Medicine, 1-20-1 Higashi-ku, Handa-yama, Hamamatsu 431-3192, Japan*
[d] *RIKEN Bio Resource Center, 3-1-1 Koyadai, Tsukuba, Ibaraki 305-0074, Japan*

ARTICLE INFO

Article history:
Available online 7 May 2008

Keywords:
Intratracheal immunization
Lentivirus
MPT51
Mycobacterium tuberculosis

ABSTRACT

The present study evaluates the potential of improved third-generation lentivirus vector with respect to their use as an *in vivo*-administered T-cell vaccine against tuberculosis. Intratracheal administration of the lentivirus vector encoding MPT51 of *Mycobacterium tuberculosis* could induce MPT51-specific CD8+ T cells in the mediastinal lymph nodes 2 weeks after the administration. The vaccination could generate MPT51-specific memory CD8+ T cells in the lung, but not in the lymph nodes. Further, a single intratracheal immunization of MPT51 lentiviral vaccine decreased significantly the number of virulent *M. tuberculosis* in the lung after intratracheal challenge of the bacillus. These findings suggest that intratracheal immunization of the third-generation lentiviral vaccines is a promising vaccination strategy against pulmonary tuberculosis.

1. Introduction

Tuberculosis (TB) has been a major cause of death by infectious diseases worldwide. There were an estimated 8.8 million new TB cases in 2005, and 1.6 million people died of TB [1]. An attenuated strain of *Mycobacterium bovis* Bacillus Calmette-Guérin (BCG) is only currently available anti-TB vaccine which is effective against the severe child forms of TB, yet its efficacy against pulmonary TB in adult is controversial [2]. It is evident that there is an urgent need for a novel and more reliable anti-TB vaccine [3].

Although the mechanisms of protection against TB have not been completely determined, cell-mediated immunity plays an important role in the control of *Mycobacterium tuberculosis* infection. There is mounting evidence that type 1 helper T cells are involved in the development of resistance to the disease, primarily through the production of macrophage-activating cytokines, such as interferon-γ (IFN-γ) [4]. In addition, CD8+ cytotoxic T-lymphocytes (CTL) contribute to disease resistance since susceptibility to *M. tuberculosis* is greater in mice deficient in CD8+ T cells [5].

Dendritic cells (DCs) are the most potent antigen-presenting cells. DCs capture bacteria and other pathogens. Then, they migrate to regional lymphoid organs, where they present antigens (Ag) to naïve T cells [6]. DCs are also known to confer T cells the ability to home to non-lymphoid sites. Activated effector/memory T cells migrate preferentially to tissues that are connected to the secondary lymphoid organs where Ag first encountered [7]. In this context, intratracheal vaccination is an attractive option to induce protective immunity against TB at the lung. In fact, *M. bovis* BCG administered via the respiratory route has been shown to be more effective than when it was given subcutaneously [8–11]. However, intratracheal administration of *M. bovis* BCG may cause severe inflammation in the trachea. For the intratracheal vaccination, such risk of adverse reactions should be avoided. The development of recombinant viral vector systems for gene therapy has prompted examination of their efficacy in gene delivery to DC and in direct immunization. Adenovirus vectors were shown to deliver Ag genes to DC. However, pre-existing immunity to viral proteins expressed by the vector prevented effective immunization [12]. Retroviral vectors based on murine leukemia virus have been employed to express Ag in DC [13]. However, the retroviral vectors only infect dividing cells.

Lentiviral vectors have been shown to efficiently transduce a variety of nondividing cells, including DC [14]. Successful

* Corresponding author: Tel.: +81 53 435 2334; fax: +81 53 435 2335.
E-mail address: koidelb@hama-med.ac.jp (Y. Koide).

0264-410X/$ – see front matter © 2008 Elsevier Ltd. All rights reserved.
doi:10.1016/j.vaccine.2008.03.101

transduction of DC with lentiviral vectors has been reported [15–17]. In addition, lentiviral vectors pseudotyped with minimal filovirus envelopes have been reported to increase gene transfer in murine lung [18]. Third-generation self-inactivating (SIN) lentiviral vector was chosen in this study because of its advanced safety profile, allowing its administration *in vivo*, and because of the presumed absence of pre-existing anti-vector immunity.

Our aim was to develop third-generation lentivirus vectors that express an *M. tuberculosis* Ag and efficiently induce cell-mediated immunity against pulmonary TB by the intratracheal instillation. As a target Ag, we employed MPT51, the protective character of which we have shown in our previous report [19].

2. Materials and methods

2.1. Mice

BALB/c mice (8–14 weeks of age; Japan SLC; Hamamatsu, Japan) were maintained in the Animal Facility of Hamamatsu University School of Medicine. All animal experiments were performed according to the Guidelines for Animal Experimentation, Hamamatsu University School of Medicine.

2.2. Lentivirus vector production

The improved third-generation lentivirus system had been developed [14,20,21]. The system comprised of following plasmids. pCAG-HIVgp is a packaging plasmid in which all accessory genes (*vif*, *vpr*, *vpu*, and *nef*) and regulatory genes (*tat* and *rev*) are deleted. pCMV-VSV-G-RSV-Rev is an expression plasmid for vesicular stomatitis virus G glycoprotein and Rev protein. The SIN plasmid, pCSII-CMV-MCS-IRES-EGFP contains a multiple cloning site and the gene encoding enhanced green fluorescent protein (EGFP). MPT51 DNA fragment was inserted into the vector, resulted in pCSII-CMV-MPT51-EGFP. The MPT51 recombinant lentivirus vector was generated by transient transfection of 293T cells with pCAG-HIVgp (10 μg), pCMV-VSV-G-RSV-Rev (10 μg), and pCSII-CMV-MPT51-EGFP (17 μg) plasmids using 10-cm dishes with DoFect-GT1 (Dojindo, Kumamoto, Japan) transfection reagent. 293T cells were cultured in Dulbecco's modified Eagle medium (DMEM; Sigma–Aldrich, St. Louis, MO, USA) containing 10% heat-inactivated fetal calf serum (FCS; Invitrogen, Carlsbad, NM, USA). Culture supernatants were collected every 24 h for 3 days, filtered through a 0.45-μm pore size filter, and concentrated two times with ultracentrifugation at 50,000 × *g* at 20 °C for 120 min. The viral supernatants were concentrated 1000 times with the ultracentrifugation, finally resuspended in sterile phosphate-buffered saline (PBS), and stored at −80 °C until use. The virus titers were determined on 293T cells by measurement of EGFP expression using flow cytometry. Titers of $1–2 \times 10^8$ infectious units (IU) ml^{-1} were usually obtained through the experiments.

2.3. Intratracheal administration

Mice were anesthetized with an intraperitoneal administration of 0.075 mg ketamine/0.015 mg xylazine per gram weight of mouse. Intratracheal administration of 5×10^6 IU of MPT51 lentivirus in 50 μl of sterile PBS was performed by infusion through the vocal cords using a fiber optic light source (LG-PS2, Olympus Optical, Tokyo, Japan) for illuminating the entrance into the trachea [22,23].

2.4. Bronchoalveolar lavage (BAL)

Mice were killed and a midline incision was made to expose the trachea. An 18-G catheter was inserted into the trachea, and the lungs were lavaged with 5 ml of ice-cold sterile PBS. Lavage cells were collected by centrifugation at 300 × *g* for 10 min at 4 °C and washed with PBS.

2.5. Lung tissue lymphocyte isolation

Lungs were removed from mice, transported in RPMI 1640 medium (5 ml per lung; Sigma–Aldrich), and cut into small pieces ($1–2\ mm^2$) with a forceps. Tissue pieces were digested with 3500 dornase units ml^{-1} of DNase I (Calbiochem, Darmstadt, Germany) and 75 units ml^{-1} of collagenase type II (Invitrogen) at 37 °C for 2 h. The digest was filtrated through a 70-μm nucleopore filter and centrifuged (300 × *g*, 10 min). The cell pellets were resuspended in PBS containing 0.01 M EDTA and chilled on ice for 5 min, and then subjected to centrifugation in Ficoll-Paque Plus solution (Amersham Pharmacia Biotech, Uppsala, Sweden) at 400 × *g* and 20 °C for 30 min. The pulmonary mononuclear cell interface was collected, washed twice, and resuspended in 5 ml of RPMI 1640 medium containing 10% FCS (RPMI/10FCS) [24].

2.6. Analysis of CD8+ T cells using MPT51 p24-32 peptide/H2-D^d tetramer complex

An MPT51 p24-32 peptide/H2-D^d tetramer complex was kindly supplied by the NIH Tetramer Facility. Cells were treated with ammonium chloride and potassium chloride (ACK) lysis buffer for 5 min at room temperature to remove erythrocytes and washed twice with RPMI 1640 medium and resuspended in RPMI/10FCS. The 1×10^6 cells were stained with phycoerythrin (PE)-conjugated MPT51 p24–32 peptide/H2-D^d tetramer complex, fluorescein isothiocyanate (FITC)-conjugated anti-CD8 (53–6.7; BD PharMingen, San Diego, CA, USA), and PE-Cy5-conjugated anti-CD4 (RM4-5; BD PharMingen) monoclonal antibodies (mAb) at 4 °C for 30 min. After washing, the cells were resuspended in PBS containing 0.1% sodium azide and 1% bovine serum albumin, and then analyzed on an EPICS digital flow cytometer (EPICS XL; Beckman Coulter, Miami, FL, USA).

2.7. Quantification of IFN-γ with cytokine enzyme-linked immunosorbent assay (ELISA)

Spleen cells were harvested from the immunized mice. Recovered cells were plated in 24-well plates at 2×10^6 cells per well in the presence or absence of 1 μM of MPT51 p24-32 peptide for 5 days. Concentration of IFN-γ in the culture supernatants was determined by a sandwich ELISA as described in our previous report [25].

2.8. Protection assay against M. tuberculosis infection

Immunized mice were subjected with intratracheal injection of 1×10^4 CFU of *M. tuberculosis* H37Rv 10 weeks after MPT51 lentivirus immunization. Mice were sacrificed 5 weeks later and the bacterial numbers in the lung were counted in CFU on Middlebrook 7H10 medium (Becton Dickinson, Sparks, MD, USA). *M. tuberculosis* H37Rv was kindly donated by Dr. Isamu Sugawara (Research Institute of Tuberculosis, Tokyo, Japan).

2.9. Statistics

Data from multiple experiments were expressed as the means ± S.D. Statistical analyses were performed by using StatView-J 5.0 statistics program (SAS Institute, Inc., Cary, NC, USA). Data were analyzed with one-factor analysis of variance followed by the Fisher's protected least significant difference (PLSD) test.

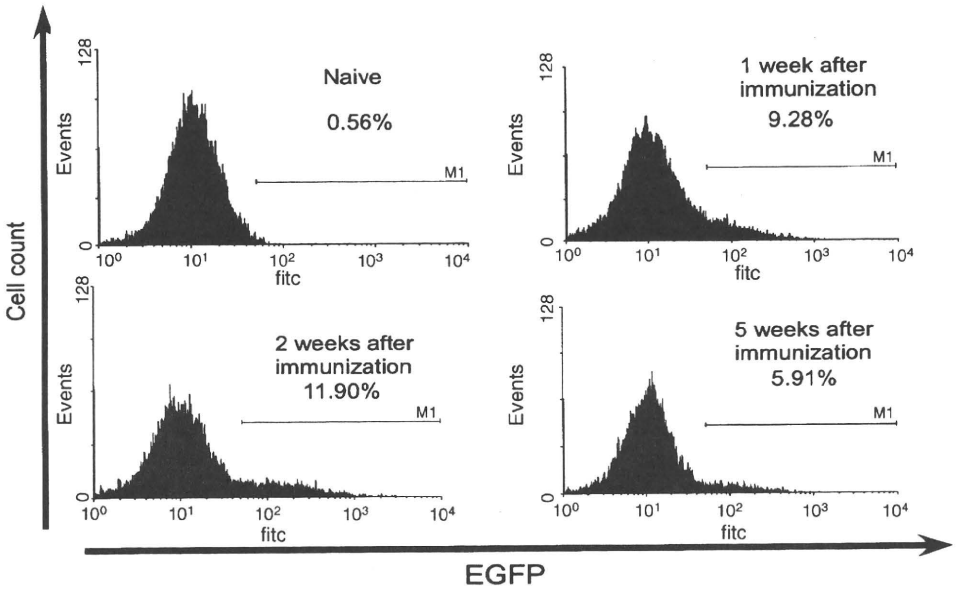

Fig. 1. EGFP expression of cells in BALF of MPT51 lentivirus-administered mice. Mice were intratracheally administered with MPT51 lentivirus and EGFP expression was measured by a flow cytometry every 1 week for 6 weeks after MPT51 lentivirus administration. Representative data are shown from three independent data which showed similar results. Percentages in the figure indicate those of EGFP-positive cells in total cells in BALF.

3. Results

3.1. EGFP expression of cells in bronchoalveolar lavage fluid (BALF) of mice intratracheally immunized with MPT51 lentivirus

The lentivirus vector used in this study was pseudotyped with vesicular stomatitis virus glycoprotein and thus was taken up through the normal endocytotic pathway. Therefore, it is able to transduce a wide variety of cells. We first examined EGFP expression of cells in BALF after intratracheal administration of MPT51 lentivirus vector vaccine. As shown in Fig. 1, EGFP expression was observed 1 week after lentivirus administration and the peak of expression was reached around 2 weeks after the administration. This observation indicates that the cells in BALF, most of which

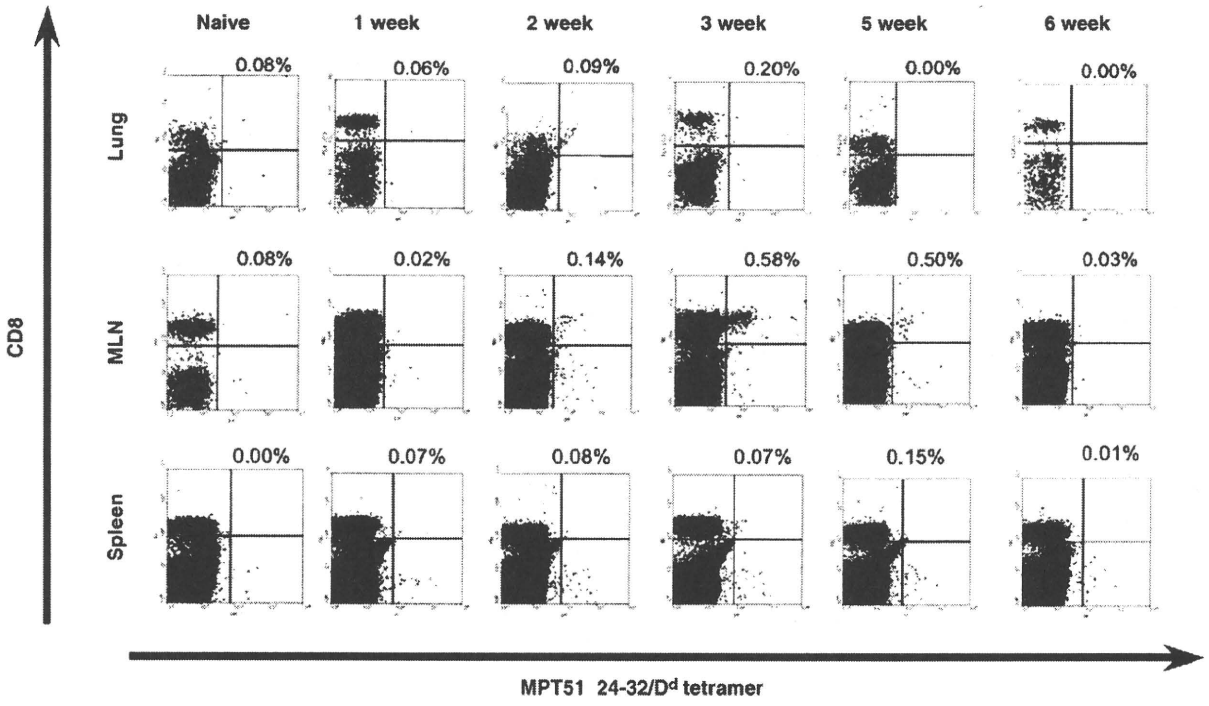

Fig. 2. MPT51 p24-32-specific CD8+ T cells in the lungs, MLN, and spleens of mice intratracheally administered with MPT51 lentivirus. Mononuclear cells were harvested from the lungs, MLN, and spleens of immunized mice and double-stained with anti-CD8 mAb and MPT51 p24-32/H2-D^d tetramer and measured by a flow cytometry. Representative data of 1–6 weeks after MPT51 lentivirus administration are shown. Percentages in the figure indicate those of tetramer-positive cells in CD8+ cells.